Sasaki H, Watanabe T, Yanai K. Neuroimaging of histamine H1-receptor occupancy in human brain by positron emission tomography (PET): a comparative study of ebastine, a second-generation antihistamine, and (+)-chlorpheniramine, a classical antihistamine. Br J Clin Pharmacol 2001; 52: 501–9.

9 Tashiro M, Sakurada Y, Iwabuchi K, Mochizuki H, Kato M, Aoki M, Funaki Y, Itoh M, Iwata R, Wong DF, Yanai K. Central effects of fexofenadine and cetirizine: measurement of psychomotor performance, subjective sleepiness, and brain histamine H1-receptor occupancy using 11C-doxepin positron emission tomography. J Clin Pharmacol 2004; 44: 890–900.

10 Tashiro M, Mochizuki H, Sakurada Y, Ishii K, Oda K, Kimura Y, Sasaki T, Ishiwata K, Yanai K. Brain histamine H receptor occupancy of orally administered antihistamines measured by positron emission tomography with (11)C-doxepin in a placebo-controlled crossover study design in healthy subjects: a comparison of olopatadine and ketotifen. Br J Clin Pharmacol 2006; 61: 16–26.

11 Ishibashi Y, Kawashima M, Harada S, Suzuki Y. [Phase I study of antiallergic agent, TAU-284 (betotastine besilate): study of inhibitory effect on intradermal reaction of histamine]. J Clin Therap Med 1997; 13: 53–63.

12 Yokota H, Mizuuchi H, Maki T, Banno K, Sato T. [Phase I study of TAU-284: single oral administration in healthy male volunteers]. J Clin Therap Med 1997; 13: 3–19.

13 Kawashima M, Harada S, Nakajima M. [Phase III study of TAU-284 (betotastine besilate) on chronic urticaria: a multicenter double blind comparative study with placebo]. J Clin Therap Med 2002; 18: 13–31.

14 Murata T, Matsumoto Y, Suzuki T, Naito K, Takata I, Tsuzurahara K. [Effect of betotastine besilate (TAU-284), a novel anti-allergic agent, on experimental allergic rhinitis]. Arerugi 1997; 46: 576–84.

15 Yato N, Murata T, Saito N, Sakai A, Kikuchi M, Tsuzurahara K, Narita H. [Anti-allergic activity of betotastine besilate (TAU-284), a new anti-allergic drug]. Nippon Yakurigaku Zasshi 1997; 110: 19–29.

16 Ueno M, Inagaki N, Nagai H, Koda A. Antiallergic action of betotastine besilate (TAU-284) in animal models: a comparison with ketotifen. Pharmacology 1998; 57: 206–14.

17 Nakahara T, Urabe K, Moroi Y, Morita K, Furue M. Bepotastine besilate rapidly inhibits mite-antigen induced immediate reactions in atopic dermatitis. J Dermatol Sci 2003; 32: 237–8.

18 Takahashi H, Ishida-Yamamoto A, Iizuka H. Effects of bepotastine, cetirizine, fexofenadine, and olopatadine on histamine-induced wheal-and flare-response, sedation, and psychomotor performance. Clin Exp Dermatol 2004; 29: 526–32.

19 Kato M, Nishida A, Aga Y, Kita J, Kudo Y, Narita H, Endo T. Pharmacokinetic and pharmacodynamic evaluation of central effect of the novel antiallergic agent betotastine besilate. Arzneimittelforschung 1997; 47: 1116–24.

20 Kay GG, Harris AG. Loratadine: a non-sedating antihistamine. Review of its effects on cognition, psychomotor performance, mood and sedation. Clin Exp Allergy 1999; 29 (Suppl. 3): 147–50.

21 Tagawa M, Kano M, Okamura N, Higuchi M, Matsuda M, Mizuki Y, Arai H, Fujii T, Komemushi S, Itoh M, Sasaki H, Watanabe T, Yanai K. Differential cognitive effects of ebastine and (+)-chlorpheniramine in healthy subjects: correlation between cognitive impairment and plasma drug concentration. Br J Clin Pharmacol 2002; 53: 296–304.

22 Hindmarch I, Shamsi Z, Kimber S. An evaluation of the effects of high-dose fexofenadine on the central nervous system: a double-blind, placebo-controlled study in healthy volunteers. Clin Exp Allergy 2002; 32: 133–9.

23 Tashiro M, Horikawa E, Mochizuki H, Sakurada Y, Kato M, Inokuchi T, Ridout F, Hindmarch I, Yanai K. Effects of fexofenadine and hydroxyzine on brake reaction time during car-driving with cellular phone use. Hum Psychopharmacol 2005; 20: 501–9.

24 Kumar S, Rurak DW, Riggs KW. Simultaneous determination of diphenhydramine, its N-oxide metabolite and their deuterium-labeled analogues in ovine plasma and urine using liquid chromatography/electrospray tandem mass spectrometry. J Mass Spectrom 1998; 33: 1171–81.

25 Kanba S, Richelson E. Histamine H1 receptors in human brain labelled with [3H]doxepin. Brain Res 1984; 304: 1–7.

26 Inoue I, Yanai K, Kitamura D, Taniuchi I, Kobayashi T, Niimura K, Watanabe T, Watanabe T. Impaired locomotor activity and exploratory behavior in mice lacking histamine H1 receptors. Proc Natl Acad Sci USA 1996; 93: 13316–20.

27 Iwata R, Pascali C, Bogni A, Miyake Y, Yanai K, Ido T. A simple loop method for the automated preparation of (11C) raclopride from (11C) methyl triflate. Appl Radiat Isot 2001; 55: 17–22.

28 Nakamura T, Hayashi Y, Watabe H, Matsumoto M, Horikawa T, Fujiwara T, Ito M, Yanai K. Estimation of organ cumulated activities and absorbed doses on intakes of several 11C labelled radiopharmaceuticals from external measurement with thermoluminescent dosimeters. Phys Med Biol 1998; 43: 389–405.

29 Fujiwara T, Watanuki S, Yamamoto S, Miyake M, Seo S, Itoh M, Ishii K, Orihara H, Fukuda H, Satoh T, Kitamura K, Tanaka K, Takahashi S. Performance evaluation of a large axial field-of-view PET scanner SET-2400w. Ann Nucl Med 1997; 11: 307–13.

30 Bergstrom M, Eriksson L, Bohm C, Blomqvist G, Litton J. Correction for scattered radiation in a ring detector positron camera by integral transformation of the projections. J Comput Assist Tomogr 1983; 7: 42–50.

31 Inoue T, Oriuchi N, Kunio M, Tomiyoshi K, Tomaru Y, Aoyagi K, Amano S, Suzuki H, Aoki J, Sato T, Endo K. Accuracy of standardized uptake value measured by simultaneous emission and transmission scanning in PET oncology. Nucl Med Commun 1999; 20: 849–57.

32 Mochizuki H, Kimura Y, Ishii K, Oda K, Sasaki T, Tashiro M, Yanai K, Ishiwata K. Simplified PET measurement for evaluating histamine H1 receptors in human brains using [11C]doxepin. Nucl Med Biol 2004; 31: 1005–11.

33 Friston KJ, Holmes AP, Worsley KJ, Poline JP, Frith CD, Frackowiak RSJ. Statistical parametric maps in functional imaging: a general linear approach. Hum Brain Mapp 1995; 2: 189–210.

34 Martinez D, Hwang D, Mawlawi O, Slifstein M, Kent J, Simpson N, Parsey RV, Hashimoto T, Huang Y, Shinn A, Van Heertum R, Abi-Dargham A, Caltabiano S, Malizia A, Cowley H, Mann JJ, Laruelle M. Differential occupancy of somatodendritic and postsynaptic 5HT (1A) receptors by pindolol: a dose-occupancy study with [11C]WAY 100635 and positron emission tomography in humans. Neuropsychopharmacology 2001; 24: 209–29.

35 Rabiner EA, Wilkins MR, Turkheimer F, Gunn RN, de Haes JU, de Vries M, Grasby PM. 5-Hydroxytryptamine1A receptor occupancy by novel full antagonist 2-[4-[4-(7-chloro-2,3-dihydro-1,4-benzdioxyn-5-yl)-1-piperazinyl]butyl]-1,2-benzisothiazol-3-(2H)-one-1,1-dioxide: a[11C][O-methyl-3H]-N-(2-(4-(2-methoxyphenyl)-1-piperazinyl) ethyl) -N-(2-py ridinyl) cyclohexanecarboxamide trihydrochloride (WAY-100635) positron emission tomography study in humans. J Pharmacol Exp Ther 2002; 301: 1144–50.

36 Talairach J, Tournoux P. Co-planar Stereotaxic Atlas of the Human Brain. Stuttgart: Georg Thieme Verlag, 1988.

37 van Rij CM, Huitema AD, Swart EL, Greuter HN, Lammertsma AA, van Loenen AC, Franssen EJ. Population plasma pharmacokinetics of 11C-flumazenil at tracer concentrations. Br J Clin Pharmacol 2005; 60: 477–85.

38 Martinez D, Broft A, Laruelle M. Imaging neurochemical endophenotypes: promises and pitfalls. Pharmacogenomics 2001; 2: 223–37.

39 Yanai K, Okamura N, Tagawa M, Itoh M, Watanabe T. New findings in pharmacological effects induced by antihistamines: from PET studies to knock-out mice. Clin Exp Allergy 1999; 29 (Suppl. 3): 29–36; discussion 37–8.

40 Yanai K, Ryu JH, Watanabe T, Iwata R, Ido T, Asakura M, Matsumura R, Itoh M. Positron emission tomographic study of central histamine H1-receptor occupancy in human subjects treated with epinastine, a second-generation antihistamine. Methods Find Exp Clin Pharmacol 1995; 17 (Suppl. C): 64–9.

41 Hindmarch I, Shamsi Z, Stanley N, Fairweather DB. A double-blind, placebo-controlled investigation of the effects of fexofenadine, loratadine and promethazine on cognitive and psychomotor function. Br J Clin Pharmacol 1999; 48: 200–6.

42 Dogan AS, Catafau AM, Zhou Y, Yanai K, Ravert H, Brasic J, Hilton J, Dannals B, Offord S, Wong DF. *In vivo* cerebral histamine receptor occupancy of three antihistamine drugs: an 11C-doxepin PET study. J Nucl Med 2001; 42: 143P–144P.

43 Ohashi R, Kamikozawa Y, Sugiura M, Fukuda H, Yabuuchi H, Tamai I. Effect of P-glycoprotein on intestinal absorption and brain penetration of antiallergic agent bepotastine besilate. Drug Metab Dispos 2006; 34: 793–9.

44 Cvetkovic M, Leake B, Fromm MF, Wilkinson GR, Kim RB. OATP and P-glycoprotein transporters mediate the cellular uptake and excretion of fexofenadine. Drug Metab Dispos 1999; 27: 866–71.

45 Nozawa T, Imai K, Nezu J, Tsuji A, Tamai I. Functional characterization of pH-sensitive organic anion transporting polypeptide OATP-B in human. J Pharmacol Exp Ther 2004; 308: 438–45.

Methods 45 (2008) 300–306

Contents lists available at ScienceDirect

Methods

journal homepage: www.elsevier.com/locate/ymeth

Application of positron emission tomography to neuroimaging in sports sciences

Manabu Tashiro [a,*], Masatoshi Itoh [a], Toshihiko Fujimoto [b], Md. Mehedi Masud [a,b], Shoichi Watanuki [a], Kazuhiko Yanai [a,c]

[a] Division of Cyclotron Nuclear Medicine, Cyclotron and Radioisotope Center, Tohoku University, Aoba 6-3, Aramaki, Aoba-ku, Sendai-shi, Miyagi-ken, Japan
[b] Center for the Advancement of Higher Education, Tohoku University, Sendai, Japan
[c] Department of Pharmacology, Graduate School of Medicine, Tohoku University, Sendai, Japan

ARTICLE INFO

Article history:
Accepted 5 May 2008
Available online 6 June 2008

Keywords:
Cerebral metabolic rate of glucose (CMRglc)
Cerebral blood flow (CBF)
[^{18}F]Fluorodeoxyglucose ([^{18}F]FDG)
Positron emission tomography (PET)
Radio-labelled water ([^{15}O]H_2O)
Exercise
Sports sciences
Neuroimaging

ABSTRACT

To investigate exercise-induced regional metabolic and perfusion changes in the human brain, various methods are available, such as positron emission tomography (PET), functional magnetic resonance imaging (fMRI), near-infrared spectroscopy (NIRS) and electroencephalography (EEG). In this paper, details of methods of metabolic measurement using PET, [^{18}F]fluorodeoxyglucose ([^{18}F]FDG) and [^{15}O]radio-labelled water ([^{15}O]H_2O) will be explained.

Functional neuroimaging in the field of neuroscience was started in the 1970s using an autoradiography technique on experimental animals. The first human functional neuroimaging exercise study was conducted in 1987 using a rough measurement system known as ^{133}Xe inhalation. Although the data was useful, more detailed and exact functional neuroimaging, especially with respect to spatial resolution, was achieved by positron emission tomography. Early studies measured the cerebral blood flow changes during exercise. Recently, PET was made more applicable to exercise physiology and psychology by the use of the tracer [^{18}F]FDG. This technique allowed subjects to be scanned after an exercise task is completed but still obtain data from the exercise itself, which is similar to autoradiography studies.

In this report, methodological information is provided with respect to the recommended protocol design, the selection of the scanning mode, how to evaluate the cerebral glucose metabolism and how to interpret the regional brain activity using voxel-by-voxel analysis and regions of interest techniques (ROI). Considering the important role of exercise in health promotion, further efforts in this line of research should be encouraged in order to better understand health behavior. Although the number of research papers is still limited, recent work has indicated that the [^{18}F]FDG-PET technique is a useful tool to understand brain activity during exercise.

1. Methodologies for functional neuroimaging on exercise

Physical exercise is executed through a sophisticated neural control system in the brain. Neural processing in the human brain plays crucial roles not only in the generation of motor outputs but also in the perception and integration of various sensory inputs. There are various methods for functional neuroimaging, such as positron emission tomography (PET) and single photon emission computed tomography, as well as other imaging methods, such as functional magnetic resonance imaging (MRI), near-infrared spectroscopy (NIRS) and electroencephalography (EEG) (Fig. 1).

We have been using PET, over the last years for measuring the regional metabolism of the brain [1,2] and skeletal muscles during exercise [3,4]. PET has been a useful tool for measuring cerebral metabolic changes induced by exercise tasks. This is especially true for PET procedures that utilize the radio-labelled glucose analogue ([^{18}F]fluorodeoxyglucose: [^{18}F]FDG). This [^{18}F]nuclide has a half-life of approximately 110 min, and such [^{18}F]labelled tracers are suitable for long observation in the range of 30–60 min. Activated regional brain activity is usually accompanied by increased demand for glucose and oxygen, which is immediately followed by dilation of brain capillaries due to increased regional cerebral perfusion (Fig. 1). Thus, cerebral perfusion can be measured using radio-labelled water ([^{15}O]H_2O), that circulates throughout the subject's body intermixed with systemic circulation so that the regions with increased perfusion show increased signals. Although PET together with [^{15}O]H_2O has been used to study brain activation during exercise, it is cumbersome and has some restrictions, that is, subjects have to exercise in the supine position during PET examinations [5–8]. This is unnatural and allows for only limited movement. Partly because of the very short half-life of [^{15}O]nuclide (approximately 2 min), the PET method using [^{15}O]H_2O is not suitable for long observation. In addition, the PET technique has the

* Corresponding author. Fax: +81 22 795 7797.
E-mail address: mtashiro@m.tains.tohoku.ac.jp (M. Tashiro).

1046-2023/$ - see front matter © 2008 Elsevier Inc. All rights reserved.
doi:10.1016/j.ymeth.2008.05.001

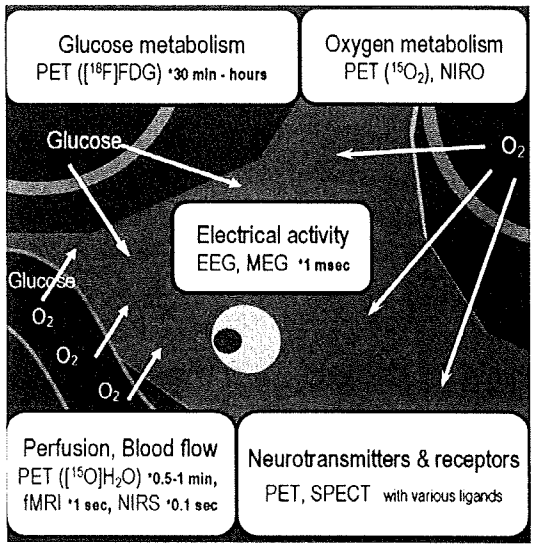

Fig. 1. Methodologies for neuroimaging and biological information obtainable from the living human brain. The most important energy resource of the human brain is glucose. Glucose metabolism can be measured using positron emission tomography (PET) with [^{18}F]fluorodeoxyglucose ([^{18}F]FDG). Temporal resolution of this method is approximately 30 min to a few hours. Oxygen is necessary for the operation of TCSA cycle to synthesize ATP molecules from glucose. Oxygen metabolism can be measured using PET with [^{15}O]O_2 and near-infrared oxymeter (NIRO). Glucose and oxygen molecules necessary for glucose metabolism are supplied by the blood flow. Brain regions with increased activity are accompanied by increased regional cerebral blood flow due to capillary dilation. At present, regional cerebral blood flow changes can be measured using various methods such as PET with [^{15}O]H_2O, functional MRI (fMRI) and near-infrared spectroscopy (NIRS). Temporal resolution of each method is 0.5–1 min, 1 s and 0.1 s, respectively. Interaction of neurotransmitters and receptors can also be measured using PET with various [^{11}C] and [^{18}F] labelled ligands.

hazard of radiation exposure and the number of repeated measurement is therefore limited, which is not the case for MRI, NIRS and EEG.

More recently, methods free from radiation exposure have been introduced. MRI (i.e., fMRI), with higher spatial and temporal resolution, has been applied to the measurement of regional perfusion alterations in the brain, though this method is more vulnerable to motion artifact compared to PET. In addition, another technique, NIRS, has also been recently introduced for measuring regional changes in brain activity, though its spatial resolution is limited and it does not measure well subcortical activation. PET measurement of regional activation using [^{15}O]H_2O is currently limited and it has been more commonly used for measuring regional brain glucose consumption and for evaluating neurotransmission function [9–12]. In this paper, the applications of PET neuroimaging in sports sciences are discussed in more detail (Fig. 1).

As mentioned above, PET has been used for measuring regional brain activity during or following exercise tasks using various radioactive pharmaceuticals such as [^{18}F]FDG and [^{15}O]H_2O. In the human brain, neurotransmitters can manifest their effects even in very small amounts. However, it is not easy to visualize their actions in the living human brain externally without using a highly sensitive technique such as PET. Although neurotransmission studies during exercise are still few, it is possible to quantify interactions between neurotransmitters and neuroreceptors in the living brain using the time course data of radioactivity in brain tissue [13].

2. A brief history of functional neuroimaging during exercise

Regional cerebral metabolic changes induced by exercise have been examined in animals using autoradiography technique such as [^{14}C]deoxyglucose ([^{14}C]2-DG) [14,15]. These studies provided the first functional indices of brain activity with respect to exercise. [^{14}C]2-DG has been a useful tracer for exercise studies because it does not require the simultaneous scanning of subjects during an exercise task [16]. Using this autoradiography technique, Sharp [17] demonstrated a selective increase in glucose uptake in the cerebellar vermis of swimming rats. On the other hand, an autoradiographic study in free-running rats showed no selective activity in the cerebellar vermis but moderately increased glucose uptake for the entire cerebellum [18].

Later, human studies were also conducted. As far as we know, the first study on human brain activity during exercise was conducted by Herholz and coworkers in 1987 [19]. In this study, subjects were examined during a riding task in the half-upright posture (about 45°) using the ^{133}Xe clearance method for studying regional changes in brain activity. They demonstrated that the largest increase in blood flow induced by an ergometer bicycle task was not in the parietal region but in the frontal region. The study had many limitations, such as low spatial resolution (a few centimeters) as well as problems with the study design. Fink and coworkers demonstrated regional activation during and immediately after an ergometer task by PET using [^{15}O]H_2O. The spatial resolution of that study was much better (around 5 mm). They showed activation in the superomedial part of the motor cortex associated with leg and arm motion, which disappeared immediately following the cessation of the motor task, while the lateral part of the motor cortex remained active possibly due to chest wall movement associated with post-exercise hyperventilation [5]. Based on the fact that muscle fibers and motor neurons jointly form "motor units", [^{18}F]FDG uptake in muscles may correlate with activity in their corresponding cerebral regions. Mishina and coworkers applied [^{18}F]FDG-PET to the neuropathological evaluation of patients with olivo-pontine-cerebellar atrophy manifesting gait disturbances who exhibited a decreased response to a walking task in the cerebellar vermis compared with normal subjects [20].

We first applied [^{18}F]FDG-PET to human subjects during a running task in the upright posture [1], and demonstrated augmented energy consumption in the parieto-occipital region during the task compared with the motor area. This was probably due to the higher energy consumption necessary for integrating multimodal sensory information. Our results also showed that frontal activity was lower during running than during resting. In addition, our study demonstrated a trend of relative decrease in whole brain mean activity during exercise compared with the resting condition. In parallel, our group also examined whole-body energy (glucose) redistribution and how exercise affects this distribution. We showed no significant changes in relative glucose metabolism in the brain between exercise and resting conditions [21]. Based on the work by Tashiro and coworkers [1], Kemppainen and coworkers examined absolute glucose consumption in the human brain of healthy volunteers. They found for the first time, using [^{18}F]FDG-PET technique, that the glucose consumption level decreases during strenuous exercise especially in the cingulate gyrus [2].

3. Measurement of cerebral glucose metabolism

The autoradiographic technique using [^{14}C]2-DG has been a useful tracer for exercise studies because it does not require simultaneous scanning of subjects during an exercise task [16]. The metabolic alteration is trapped, which enables the observation of the remaining metabolic "record" or "memory" afterward. With this technique, data acquisition can be performed following exercise tasks although the data "dates back" to the exercise itself. However, the [^{14}C]2-DG is not applicable to human activation studies because its half-life is too long. Mishina and coworkers measured

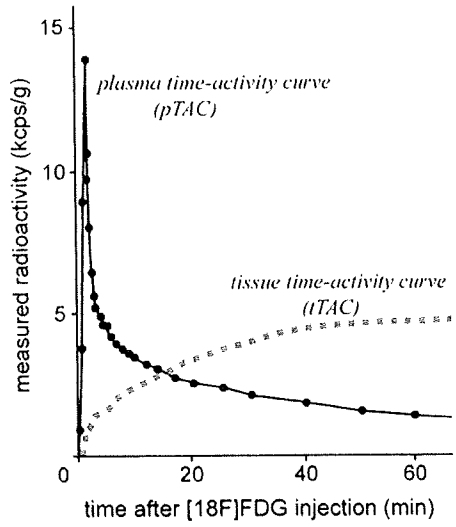

Fig. 2. Time–activity curves in plasma (pTAC: solid line) and tissue (tTAC: dotted line) following [^{18}F]FDG injection. The plasma concentration of [^{18}F]FDG is very high for the first 10 min or so after injection, and then gradually decreases. Therefore, it is recommended that exercise tasks be completed within the first 30 min or so. [^{18}F]FDG accumulation in the tissue (brain) reaches a plateau after 30–40 min following injection. A prolonged exercise task lasting for 60 min after injection does not produce additional accumulation since the plasma concentration of [^{18}F]FDG is already very low; instead, blood with low [^{18}F]FDG concentration might wash out the FDG particularly after 60 min of injection. Abbreviation: kcps, kilo-count per second.

cerebellar glucose uptake before and after walking in patients with neurological disorders using [^{18}F]FDG [20]. Although their main purpose was the clinical evaluation of a specific neurological disorder, this is probably the first study conducted in human subjects to investigate the effect of actual walking on brain activity. Thus, [^{18}F]FDG has proven to be an ideal tracer for exercise physiology studies in humans because of its metabolic trapping property, a property that has already been recognized together with [^{14}C]2-DG, for that purpose. When this tracer is used, the [^{18}F]FDG molecules are taken up by activated regional brain or muscle tissues in proportion to the energy consumption level of these tissues. Then, the [^{18}F]FDG molecules are phosphorylated in a manner similar to a glucose molecule. However, these [^{18}F]FDG molecules escape from further metabolism and are eventually trapped in the tissue, preserving the metabolic pattern for an hour or so [16]. Thus, it is possible to estimate energy consumption in different regions of the brain an hour after the completion of physical activity.

As shown in Fig. 2, the plasma time–activity curve (pTAC) demonstrates that the plasma [^{18}F]FDG concentration is very high for the first 10 min or so after injection, and then gradually decreases. Therefore, it is recommended that some kind of exercise tasks be conducted during the first 30 min or so. A prolonged exercise task up to 60 min after injection would not produce much difference since the plasma [^{18}F]FDG concentration is already very low. Instead, the blood with low [^{18}F]FDG concentration might wash out the [^{18}F]FDG particularly 60 min after injection. With this in mind, [^{18}F]FDG-PET can be an ideal technique for studies on exercise physiology by separating "a task phase" (the first 30 min or so) and "data acquisition phase" (30–60 min after injection). This paradigm allows investigation of a totally free movement task assigned to subjects. NIRS also allows observation of moving subjects; however, the subjects are connected to the data acquisition system by a measurement cap and cables, requiring proximity to the system for any tasks to be performed. Also, it is prone movement artifacts for gross movements. With the [^{18}F]FDG-PET technique, subjects can carry out any tasks, that is, not only running but any movement such as driving of a car or swimming [22]. Thus, although the temporal resolution of the [^{18}F]FDG-PET technique is limited (just 30–60 min), it is exactly this unique property that enables the application of this technique to human movement science.

As for the cellular and molecular mechanism of the [^{18}F]FDG-PET and autoradiography techniques, new studies have added several novel findings. Brain glucose/[^{18}F]FDG was thought to be transported and consumed by neural cells. However, recent studies have demonstrated that glucose/[^{18}F]FDG is transported through the blood–brain barrier (BBB) to be taken up by astrocytes, which express a large number of glucose transporters (GLUT) of GLUT-1 type on their surface membranes. It has been proposed that neurons receive their energy source from these astrocytes in the form of lactate produced by glycolysis and lactate dehydrogenase action [23–25]. Magistretti and Pellerin have established the "astrocyte-neuron lactate shuttle hypothesis" (ANLSH), an operational model for the coupling between synaptic activity and glucose utilization. This model seems to be consistent with the notion that the signals detected during brain activation studies using [^{18}F]FDG-PET may predominantly reflect tracer uptake not into neurons but into astrocytes [23–25]. This theory has provided a cellular and molecular basis for these functional brain imaging techniques; however, it does not question the validity of brain activation techniques using [^{18}F]FDG and [^{14}C]2-DG [23–25].

4. Data acquisition and two- and three-dimensional modes

PET is the method of choice for functional imaging using radiopharmaceuticals that detect annihilation photons with relatively high energy (511 keV) emitted from injected radioisotopes. Recent technical advances have allowed the development of a new three-dimensional (3D) data acquisition mode system with increased sensitivity of up to about 8–10 times that of a conventional two-dimensional (2D) mode system [26]. This significant increase in sensitivity has lead to a substantial reduction in radiological doses and therefore reduction in radiation exposure to subjects. With this innovation, studies on healthy volunteers using PET have become more feasible than before. Thus, we first applied this technique to map changes in whole-body glucose metabolism during running in the upright posture [3], and assessed skeletal muscle activity in normal healthy volunteers [4]. Usually, [^{18}F]FDG of 190–370 MBq (5–10 mCi) is injected to patients for clinical diagnosis using 2D acquisition mode. Since the effective doses in humans using [^{18}F]FDG is estimated as 0.02 mSv/MBq or so (0.8 mSv/mCi or so) [27], the radiation exposure to the patients is estimated to be 3.8–7.4 mSv. Using the 3D acquisition mode, 40–80 MBq (1–2 mCi) would be enough for the exercise study however. Thus the radiation exposure to the subjects is far below (0.8–1.6 mSv) the annual accumulated environmental radiation exposure (2.4 mSv). Thus, for safety reasons in terms of radiation, it is recommended to use the 3D acquisition mode for exercise study because it allows for less radiation exposure to otherwise healthy subjects. In addition, depending on the study protocol, a practical way to minimize radiation exposure would be to avoid scanning the same subject more than twice.

5. Protocols for measuring cerebral glucose metabolism during exercise

At many institutes, [^{18}F]FDG is presently synthesized based on the procedure introduced by Hamacher and colleagues [28]. In studies using [^{18}F]FDG, it is expected that all subjects refrain from eating and drinking for at least for 3–4 h before starting the examinations ([^{18}F]FDG injection). If possible, fasting for 5 h would be

ideal because the influx of [^{18}F]FDG molecules into the brain tissue is affected by plasma glucose level, and an increased level of plasma glucose lowers [^{18}F]FDG uptake into the brain because of competition. Thus, plasma glucose concentration should be measured in all subjects just prior to [^{18}F]FDG injection to determine if the glucose level is within the appropriate range. Moreover, subjects should not perform any exercise one day before the examinations. In a previous study by Kemppainen and coworkers, subjects fasted for at least 12 h before the study and any kind of strenuous physical activity was prohibited for at least one day before PET examination [2]. Usually, PET scanning is initiated 40 min after [^{18}F]FDG injection since [^{18}F]FDG uptake in brain tissue reaches the plateau level at around 40–50 min post-injection. Also, it is recommended to recruit subjects who are all right-handed or left-handed because some studies have suggested effects of lateralization of specific sensori-motor functions [29,30]. Our previous study suggested the presence of lateralization in muscular glucose metabolism used during upright running [1].

Usually, subjects are instructed to run for a total of 30–40 min after [^{18}F]FDG injection, with 10–15 min of exercise before injection. The amount of injected [^{18}F]FDG is approximately 40–80 MBq (1–2 mCi per subject) if a 3D data acquisition system is used. If a 2D system is used, 200 MBq [^{18}F]FDG (approximately 5 mCi) is needed for data acquisition to compensate for the lower sensitivity of the detector system. For [^{18}F]FDG injection, a catheter is usually inserted into an antecubital forearm vein. For quantification of absolute glucose consumption rate, another catheter should be, in principle, inserted in the artery of the opposite arm for serial sampling of arterial blood. Some investigators also use arterialized venous blood data using the opposite antecubital vein. In this case, the forearm should be warmed so that as many arterio-venous shunts are opened as possible. In order to observe "relative" cerebral glucose metabolic changes, however, investigators do not have to carry out serial blood sampling.

Following an exercise task, PET scanning is initiated. There are two kinds of scanning modes, namely, "emission" and "transmission" scans. In emission scanning, annihilation photons (gamma rays of 511 keV) emitted from the injected radiopharmaceuticals in the body of subjects are detected by the PET detector system. In transmission scanning, external radiation sources such as ^{68}Ge/^{68}Ga emitting 511 keV gamma rays are detected by PET detectors to map the tissue attenuation throughout the brain. These transmission data are used for correcting the emission data affected by tissue attenuation [26]. As indicated in Fig. 4, the deeper the location of the brain structure, the more the counts are attenuated due to absorption and diffraction in the brain and surrounding tissues. For the data analysis, images corrected for tissue attenuation should be used.

6. Quantification of cerebral metabolic rate of glucose

Quantification of regional cerebral metabolic rate of glucose (rCMRglc) is done based on the method developed by Sokoloff and coworkers, who used the equation below based on a compartment model consisting of three compartments for "[^{18}F]FDG in plasma", "unmetabolized [^{18}F]FDG in the brain" and "metabolized [^{18}F]FDG in the brain", as shown in Fig. 3 [31,32]:

$$\mathrm{CMRglc} = \frac{C_p}{\mathrm{LC}}\left[\frac{k_1^* k_3^*}{k_2^* + k_3^*}\right]\left[\frac{C_i^*(T) - C_e^*(T)}{C_m^*(T)}\right]$$

where C_p denotes native glucose concentration in plasma, LC denotes the lumped constant for [^{18}F]FDG, k_1^* to k_3^* denote the first order kinetic rate constants for [^{18}F]FDG, $[C_i^*(T) - C_e^*(T)]/C_m^*(T)$ is the factor that corrects the ratio between observed and the population-average metabolic rates [31,32]. For the calculation of

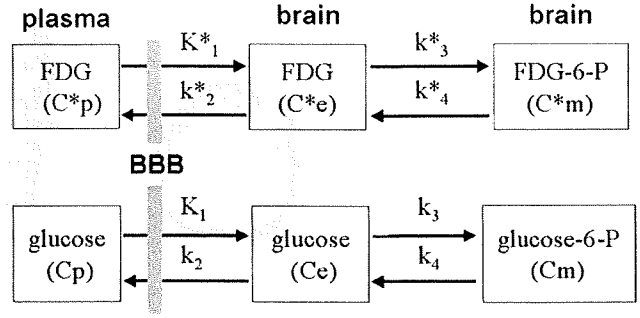

Fig. 3. Schematic diagram demonstrating the kinetic model for quantification of regional cerebral metabolic rate of glucose (rCMRglc). This compartment model consists of three compartments for "FDG in plasma", "unmetabolized FDG in the brain" and "metabolized FDG in the brain". C_p, C_e and C_m denote concentrations of native glucose in plasma and the brain tissue, and metabolized glucose (glucose 6-phosphate, glucose-6-P), respectively. C_p^*, C_e^* and C_m^* denote concentrations of FDG in plasma and the brain tissue, and metabolized FDG (FDG 6-phosphate, FDG-6-P), respectively. k_1 to k_4 denote the first-order kinetic rate constants for glucose. k_i^* to k_4^* denote the first-order kinetic rate constants for FDG. Abbreviation: BBB, blood–brain barrier.

rCMRglc, LC of 0.52, reported by Reivich and coworkers, is often used [33]. Recently, Wakita and coworkers established a simplified quantification technique using 1-point blood sampling data using arterial (12 min after injection) and venous (40 min after injection) blood [34]. In addition to the method for quantifying rCMRglc based on the full kinetic model [35,36], simplified graphical analytic methods are also available. The latter is used in PET scans performed after exercise (lacking the first part of the time–activity curve), as reported in the study by Kemppainen and coworkers [2]. In the first quantification study conducted by Kemppainen and coworkers, plasma radioactivity tended to be low 25 min after tracer injection and exercise. This suggests that the period between the end of exercise and the start of the scan had a minor effect on cerebral tissue tracer counts [2], which indicated that the measured k_i reflects the existing condition during exercise.

In addition to the determination of rCMRglc, rough estimation of [^{18}F]FDG distribution is also sometimes used to identify changes in global mean glucose metabolism. Tashiro and coworkers previously calculated the modified standardized uptake ratio (SUR) (also known as standardized uptake value, SUV), which represents the ratio of the global mean cerebral glucose uptake to the whole body [^{18}F]FDG uptake, using the following equation:

$$\mathrm{SURm} = \frac{\text{global mean cerebral [}^{18}\text{F]FDG uptake per volume (cps/pixel)}}{\text{mean whole body [}^{18}\text{F]FDG uptake per volume (cps/pixel)}}$$

A basic equation is introduced by Kubota and coworkers as follows [37]:

$$\mathrm{SUR} = \frac{[^{18}\text{F]FDG uptake per volume (cps/pixel)} * \text{body size of subjects (kg)}}{\text{injected dose(MBq)} * \text{calibration factor(cps/MBq)}}$$

7. Voxel-by-voxel analysis using statistical parametric mapping

Voxel-by-voxel analysis is the standard tool in detecting changes in activity levels in certain brain regions. The most popular contrast in exercise studies has been to contrast "resting" with "active exercise". In addition, voxel-by-voxel analysis as been useful in detecting brain regions correlating with specific cofounding factors such as age, exercise intensity, as well as measures of blood chemistry and autonomic nervous function. As demonstrated in previous exercise studies [1,2], the most popular software tool for this analysis has been the "Statistical Parametric Mapping (SPM)" software package.

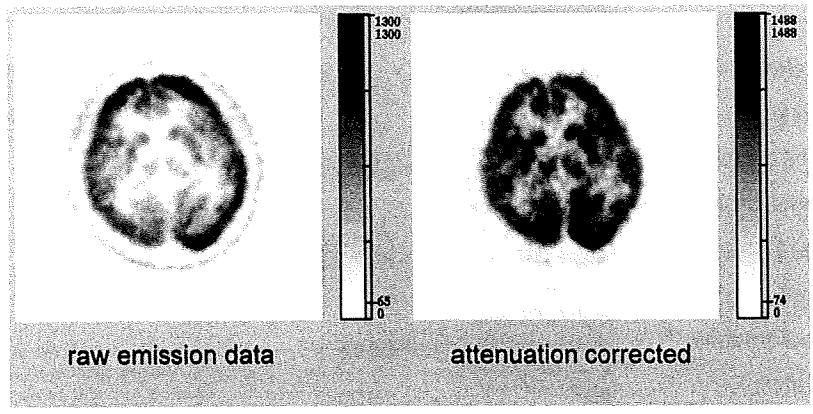

Fig. 4. Brain images with and without attenuation correction. Rawemission data (LEFT) have low signals in the middle part of the brain due to increased tissue attenuation. This tissue attenuation can be corrected using transmission data. The corrected image is shown in the right hand of this figure.

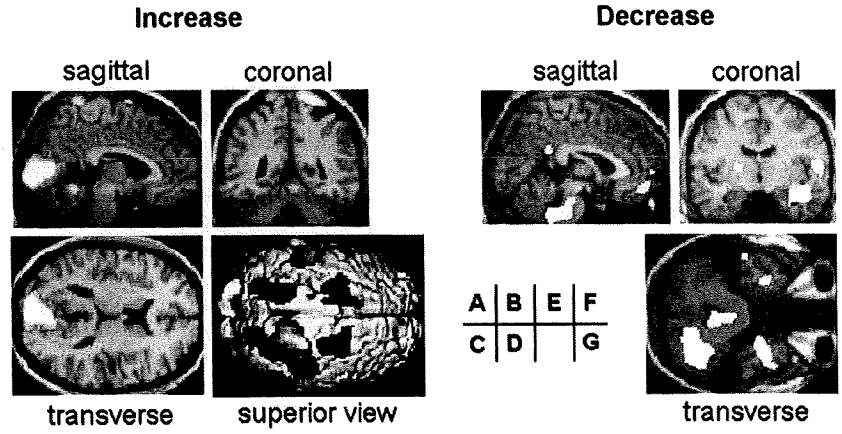

Fig. 5. Voxel-by-voxel analysis can visualize both increased and decreased regional brain activities associated with exercise task. Areas of significantly increased (LEFT) and decreased (RIGHT) glucose metabolisms during running, where the areas with statistically-significant changes appear in red to yellow. Sagittal section image (A) showing high glucose uptake in the posterior parietal, occipital visual and premotor cortices, and cerebellar vermis. Coronal section image (B) showing high uptake in the posterior parietal cortex and cerebellar vermis. Transverse sectional image (C) showing high uptake in the occipital visual cortex. Surface rendering image providing superior (vertex) view which demonstrates high uptake in the premotor, temporo-parieto-occipital association and visual cortices (D). Sagittal section image (E) on the right showing low uptake in the basal prefrontal cortex. Coronal section image (F) showing low uptake in the temporal lobe including the basal ganglia. Transverse section image (G) showing low uptake in the cerebellar hemisphere and inferoanterior temporal regions. Modified from the Ref. [1] by courtesy of Minerva Medica.

Briefly, the brain parametric images of each individual are realigned across different conditions using parameters estimated from summed images. For statistical analysis, all brain images were anatomically normalized by mathematical calculation including linear and non-linear transformations to minimize inter-subject anatomical variation using the SPM software package [38]. This normalization procedure is executed based on MRI T1 image of each subject's own or a ligand-specific template for [^{18}F]FDG that is available from the SPM site. In the work by Kemppainen et al. [2], the brain images were then smoothed using a 12- to 16-mm isotropic Gaussian kernel to increase the signal-to-noise ratio, depending on the spatial resolution of the PET scanner. For statistical analysis, all pixel values were normalized to an arbitrary global mean value of 50 mg/100 ml/min by ANCOVA to exclude the effects of inter-subject variability in global cerebral glucose metabolism. The paired *t*-test was applied to each voxel; only voxel clusters were maintained with voxels corresponding to $p < 0.001$ in a single test and a cluster size of 8 voxel minimum in two ways (runners-controls and controls-runners) [39]. The statistical significance of a regional metabolic change was given in Z scores. Empirically in SPM analysis, a Z score higher than 3.0 (approximately corresponding to $p < 0.001$) is roughly considered as statistically significant. The location of each statistical peak was identified based on a co-planar stereotaxic atlas of the human brain [40]. Recently, this localization procedure is often carried out using the MNI Space utility, which first converts the MNI coordinates given by SPM to Talairach coordinates using non-linear transformation and then identifies each voxel by the anatomical labels presented in the Talairach Daemon database [41]. Statistically significant areas were superimposed on the standard MRI brain template images (Fig. 5). The adjusted regional metabolic rate ratio at each statistical peak is available by defining regions of interest (ROIs) based on the normalized brain images as demonstrated by the plotted data in Fig. 6 [39]. In principle, the SPM analysis is conducted as an explorative analysis covering the whole brain, that is, without any *a priori* hypothesis or spatial constrictions concerning the location of potential effects. If carried out with a certain *a priori* hypothesis or spatial constrictions concerning the location of potential effects, statistical thresholds can be lowered. In addition, in case the quantitative brain images of glucose metabolic rate (GMR) values are used, SPM analyses should be performed without global normalization function.

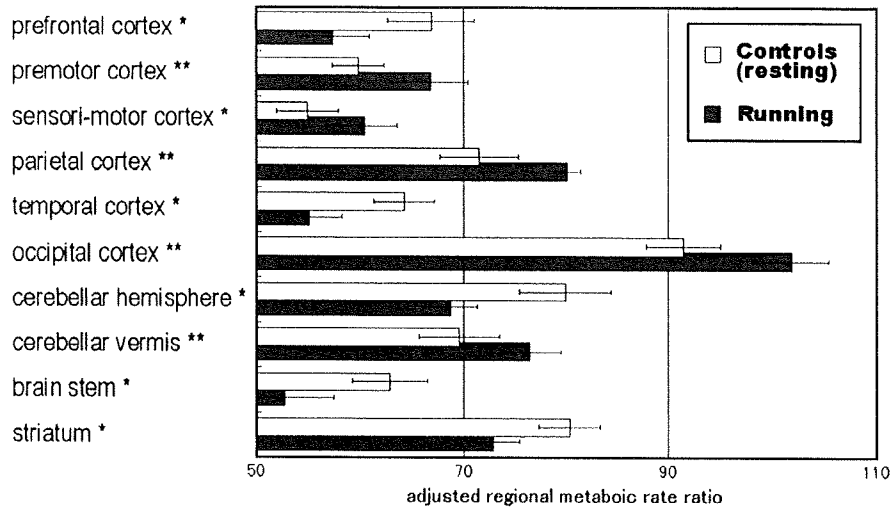

Fig. 6. Relative glucose metabolic differences between Controls (resting) and Running subjects demonstrated in terms of adjusted regional glucose metabolic rate ratios. Brain regions of statistically significant difference are shown in this figure. In all areas, $p < 0.001$, compared Controls (resting) and Running subjects. Symbols: "Z score >4.0, 'Z > 3.0. Modified from Ref. [1] by courtesy of Minerva Medica.

8. Regions of interest (ROIs) analysis

Activation in specific brain regions is associated with a certain task. For exercise, these are the motor cortex, premotor cortex, striatum, cerebellum, and a host of sensory and automatic systems. Investigators might have even specific *a priori* hypotheses regarding a specific neural network. In such cases, it is possible to examine the regional brain activity directly. The most exact and reliable way to do this analysis is to first coregister as a reference the PET image to the MRI T1 image of the same subject. Then, the investigators can directly analyze the glucose consumption of specific brain regions.

An automated ROI analysis is also available. This enables the reliable quantitative estimation of rGMR values when SPM only gives the significance of the difference in rGMR values [42]. In this method, standardized ROIs are defined on a mean MRI template image representing the brain anatomy in accordance with the Montreal Neurological Institute (MNI) space. As this method is based on a common stereotactic space (i.e., spatially normalized parametric images), operator-induced errors in defining ROIs individually for each subject can be avoided. The ROIs can be defined on the mean MRI template, there, as in the study by Kemppainen et al. [2].

9. What the study results mean

Using [^{18}F]FDG-PET technique, Tashiro and coworkers have demonstrated the relative increase in glucose uptake in the temporo-parietal association cortex, occipital cortex, premotor cortex, primary sensorimotor cortex and the cerebellar vermis [1]. Relative reduction of glucose uptake was detected in the prefrontal cortex, temporal cortex, cerebellar hemisphere, brain stem and striatum. Mean values of global brain glucose uptake was relatively lower in runners than in resting controls [1]. Kemppainen and coworkers also demonstrated significant reduction of regional glucose metabolic rate in all cortical regions in correlation to exercise intensity, especially in the dorsal part of the anterior cingulate cortex [2]. Interestingly, they also pointed out that exercise training could be related to adaptive metabolic changes in the frontal cortex [2]. Thus, global and regional brain metabolic decline was observed using [^{18}F]FDG-PET especially in the limbic and frontal regions [1,2]. It is easy to explain the metabolic increase in the regions directly associated with execution of exercise task, while it is not so easy to explain the mechanism of relative decrease in the regions not involved in exercise. The relatively low glucose uptake detected in the cerebellar hemisphere in the study by Tashiro and coworkers was brought about by the adaptation due to the repetition of the same motor task [9], while the cause of the reduced metabolism in the prefrontal cortex and limbic regions was not known at that moment. Previous imaging studies in anxiety disorders demonstrated increased glucose metabolism in these regions [43,44]. We speculated that the frontal and limbic hypometabolism was associated with emotional changes in runners, including the phenomenon called "runner's high", a sensation of well-being and reduced anxiety during running [45].

Dietrich and Sparling reported that endurance exercise tended to impair prefrontal-dependent cognitive ability in healthy young male volunteers [46]. Based on this finding and others, Dietrich has proposed a new theory to explain the hypometabolism especially in the prefrontal region [47]. According to Dietrich's transient hypofrontality theory (THT), the prefrontal activity is suppressed indirectly due to the limitation in energy supply to the brain through blood in the situation where enormous amount of energy is needed for execution of endurance exercise [47]. Interestingly, this theory also explains a neural mechanism regarding the mental health benefits of exercise [46,47]. Here, it is of interest to also point out that Kemppainen and coworkers have suggested that substrates other than glucose, most likely lactate, are used by the brain as energy source in order to compensate the increased energy demand to maintain neuronal activity during high intensity exercise, since lactate availability during exercise tended to correlate negatively with the brain glucose uptake measured with [^{18}F]FDG-PET in their study [2].

10. Conclusion

PET neuroimaging in the field of sports science is a relatively new research field. An advantage of [^{18}F]FDG-PET method is that subjects do not have to be scanned at the same time than during the exercise. We showed the feasibility of using FDG-PET in monitoring relative changes in the activity of different brain regions induced by running. This technique supplies further evidence to support the positive aspects of exercise in the fields of sports

physiology and psychology. We anticipate that this technique would become a useful tool in sports medicine in the investigation of human physiological and psychological response to exercise.

Acknowledgments

The authors thank the support of all the staff of the Cyclotron and Radioisotope Center, Tohoku University, for their support during the study. This report was in part supported by Grants-in-Aid for Scientific Research (Nos. 19650157 for M.T., 16650150, 14704059 for T.F., and 17390156 for K.Y.) from the Japan Society of Promotion of Science (JSPS) and the Ministry of Education, Culture, Sports, Science and Technology in Japan, as well as by a Grant from the Japan Society of Technology (JST) on research and education in "molecular imaging".

References

[1] M. Tashiro, M. Itoh, T. Fujimoto, T. Fujiwara, H. Ota, K. Kubota, M. Higuchi, N. Okamura, K. Ishii, D. Bereczki, H. Sasaki, J. Sports Med. Phys. Fitness 41 (2001) 11–17.
[2] J. Kemppainen, S. Aalto, T. Fujimoto, K.K. Kalliokoski, J. Langsjo, V. Oikonen, J. Rinne, P. Nuutila, J. Knuuti, J. Physiol. 568 (2005) 323–332.
[3] T. Fujimoto, M. Itoh, H. Kumano, M. Tashiro, T. Ido, Lancet 348 (1996) 266.
[4] M. Tashiro, T. Fujimoto, M. Itoh, K. Kubota, T. Fujiwara, M. Miyake, S. Watanuki, E. Horikawa, H. Sasaki, T. Ido, J. Nucl. Med. 40 (1999) 70–76.
[5] G.R. Fink, L. Adams, J.D. Watson, J.A. Innes, B. Wuyam, I. Kobayashi, D.R. Corfield, K. Murphy, T. Jones, R.S. Frackowiak, et al., J. Physiol. 489 (Pt 3) (1995) 663–675.
[6] J.W. Williamson, A.C. Nobrega, R. McColl, D. Mathews, P. Winchester, L. Friberg, J.H. Mitchell, J. Physiol. 503 (Pt. 2) (1997) 277–283.
[7] J.G. Colebatch, M.P. Deiber, R.E. Passingham, K.J. Friston, R.S. Frackowiak, J. Neurophysiol. 65 (1991) 1392–1401.
[8] K.J. Friston, C.D. Frith, R.E. Passingham, P.F. Liddle, R.S. Frackowiak, Proc. Biol. Sci. 248 (1992) 223–228.
[9] M. Tashiro, Y. Sakurada, K. Iwabuchi, H. Mochizuki, M. Kato, M. Aoki, Y. Funaki, M. Itoh, R. Iwata, D.F. Wong, K. Yanai, J. Clin. Pharmacol. 44 (2004) 890–900.
[10] M. Higuchi, M. Tashiro, H. Arai, N. Okamura, S. Hara, S. Higuchi, M. Itoh, R.W. Shin, J.Q. Trojanowski, H. Sasaki, Exp. Neurol. 162 (2000) 247–256.
[11] X.S. Hu, N. Okamura, H. Arai, M. Higuchi, T. Matsui, M. Tashiro, M. Shinkawa, M. Itoh, T. Ido, H. Sasaki, Neurology 55 (2000) 1575–1577.
[12] N. Okamura, Y. Funaki, M. Tashiro, M. Kato, Y. Ishikawa, M. Maruyama, H. Ishikawa, K. Meguro, R. Iwata, K. Yanai, Br. J. Clin. Pharmacol. 65 (2008) 472–479.
[13] G.J. Wang, N.D. Volkow, J.S. Fowler, D. Franceschi, J. Logan, N.R. Pappas, C.T. Wong, N. Netusil, J. Nucl. Med. 41 (2000) 1352–1356.
[14] M. Reivich, L. Sokoloff, H. Shapiro, M. des Rosiers, C. Kennedy, Trans. Am. Neurol. Assoc. 99 (1974) 238–240.
[15] R.J. Schwartzman, J. Greenberg, M. Revich, K.J. Klose, G.M. Alexander, Exp. Neurol. 72 (1981) 153–163.
[16] B.M. Gallagher, J.S. Fowler, N.I. Gutterson, R.R. MacGregor, C.N. Wan, A.P. Wolf, J. Nucl. Med. 19 (1978) 1154–1161.
[17] F.R. Sharp, Brain Res. 110 (1976) 127–139.
[18] J. Vissing, M. Andersen, N.H. Diemer, J. Cereb. Blood Flow Metab. 16 (1996) 729–736.
[19] K. Herholz, W. Buskies, M. Rist, G. Pawlik, W. Hollmann, W.D. Heiss, J. Neurol. 234 (1987) 9–13.
[20] M. Mishina, M. Senda, K. Ishii, M. Ohyama, S. Kitamura, Y. Katayama, Acta Neurol. Scand. 100 (1999) 369–376.
[21] M. Iemitsu, M. Itoh, T. Fujimoto, M. Tashiro, R. Nagatomi, H. Ohmori, K. Ishii, Med. Sci. Sports Exerc. 32 (2000) 2067–2070.
[22] M. Jeong, M. Tashiro, L.N. Singh, K. Yamaguchi, E. Horikawa, M. Miyake, S. Watanuki, R. Iwata, H. Fukuda, Y. Takahashi, M. Itoh, Ann. Nucl. Med. 20 (2006) 623–628.
[23] P.J. Magistretti, L. Pellerin, Ann. NY Acad. Sci. 777 (1996) 380–387.
[24] P.J. Magistretti, L. Pellerin, News Physiol. Sci. 14 (1999) 177–182.
[25] L. Pellerin, A.K. Bouzier-Sore, A. Aubert, S. Serres, M. Merle, R. Costalat, P.J. Magistretti, Glia 55 (2007) 1251–1262.
[26] T. Fujiwara, S. Watanuki, S. Yamamoto, M. Miyake, S. Seo, M. Itoh, K. Ishii, H. Orihara, H. Fukuda, T. Satoh, K. Kitamura, K. Tanaka, S. Takahashi, Ann. Nucl. Med. 11 (1997) 307–313.
[27] G. Brix, U. Lechel, G. Glatting, S.I. Ziegler, W. Munzing, S.P. Muller, T. Beyer, J. Nucl. Med. 46 (2005) 608–613.
[28] K. Hamacher, H.H. Coenen, G. Stocklin, J. Nucl. Med. 27 (1986) 235–238.
[29] S.F. Walker, Br. J. Psychol. 71 (1980) 329–367.
[30] R.C. Leiguarda, Adv. Neurol. 93 (2003) 235–248.
[31] L. Sokoloff, M. Reivich, C. Kennedy, M.H. Des Rosiers, C.S. Patlak, K.D. Pettigrew, O. Sakurada, M. Shinohara, J. Neurochem. 28 (1977) 897–916.
[32] M.E. Phelps, S.C. Huang, E.J. Hoffman, C. Selin, L. Sokoloff, D.E. Kuhl, Ann. Neurol. 6 (1979) 371–388.
[33] M. Reivich, D. Kuhl, A. Wolf, J. Greenberg, M. Phelps, T. Ido, V. Casella, J. Fowler, B. Gallagher, E. Hoffman, A. Alavi, L. Sokoloff, Acta Neurol. Scand. Suppl. 64 (1977) 190–191.
[34] K. Wakita, Y. Imahori, T. Ido, R. Fujii, H. Horii, M. Shimizu, S. Nakajima, K. Mineura, T. Nakamura, T. Kanatsuna, J. Nucl. Med. 41 (2000) 1484–1490.
[35] L. Sokoloff, Trends Neurosci. 1 (1978) 75–79.
[36] K. Wienhard, Methods 27 (2002) 218–225.
[37] K. Kubota, T. Matsuzawa, M. Ito, K. Ito, T. Fujiwara, Y. Abe, S. Yoshioka, H. Fukuda, J. Hatazawa, R. Iwata, et al., J. Nucl. Med. 26 (1985) 37–42.
[38] K.J. Friston, C.D. Frith, P.F. Liddle, R.S. Frackowiak, J. Cereb. Blood Flow Metab. 11 (1991) 690–699.
[39] K.J. Friston, A.P. Holmes, K.J. Worsley, J.P. Poline, C.D. Frith, R.S.J. Frackowiak, Hum. Brain Mapp. 2 (1995) 189–210.
[40] J. Talairach, P. Tournoux, Co-planar Stereotaxic Atlas of the Human Brain, Georg Thieme Verlag, Stuttgart, Germany, 1988.
[41] J.L. Lancaster, M.G. Woldorff, L.M. Parsons, M. Liotti, C.S. Freitas, L. Rainey, P.V. Kochunov, D. Nickerson, S.A. Mikiten, P.T. Fox, Hum. Brain Mapp. 10 (2000) 120–131.
[42] A.S. Nagano, K. Ito, T. Kato, Y. Arahata, T. Kachi, K. Hatano, Y. Kawasumi, A. Nakamura, T. Yamada, Y. Abe, T. Ishigaki, Neuroimage 11 (2000) 760–766.
[43] L.R. Baxter, J. Clin. Psychiatry (51 Supp) (1990) 22–25. discussion 26.
[44] D. Perani, C. Colombo, S. Bressi, A. Bonfanti, F. Grassi, S. Scarone, L. Bellodi, E. Smeraldi, F. Fazio, Br. J. Psychiatry 166 (1995) 244–250.
[45] Boecker, H., Sprenger, T., Spilker, M.E., Henriksen, G., Koppenhoefer, M., Wagner, K.J., Valet, M., Berthele, A., Tolle, T.R., 2008. Cereb. Cortex in press.
[46] A. Dietrich, P.B. Sparling, Brain Cogn. 55 (2004) 516–524.
[47] A. Dietrich, Psychiatry Res. 145 (2006) 79–83.

American Journal of Gastroenterology
© 2008 by Am. Coll. of Gastroenterology
Published by Blackwell Publishing

ISSN 0002-9270
doi: 10.1111/j.1572-0241.2008.02066.x

Contributions of Pain Sensitivity and Colonic Motility to IBS Symptom Severity and Predominant Bowel Habits

Motoyori Kanazawa, M.D., Ph.D.,[1,2] Olafur S. Palsson, Psy.D.,[1] Syed I.M. Thiwan, M.D.,[1] Marsha J. Turner, M.S.,[1] Miranda A.L. van Tilburg, Ph.D.,[1] Lisa M. Gangarosa, M.D.,[1] Denesh K. Chitkara, M.D.,[1] Shin Fukudo, M.D., Ph.D.,[2] Douglas A. Drossman, M.D.,[1] and William E. Whitehead, Ph.D.[1]

[1]*Center for Functional GI and Motility Disorders, University of North Carolina at Chapel Hill, Chapel Hill, North Carolina; and* [2]*Department of Behavioral Medicine, Tohoku University Graduate School of Medicine, Sendai, Japan*

OBJECTIVES: **Irritable bowel syndrome (IBS) patients show pain hypersensitivity and hypercontractility in response to colonic or rectal distention. Aims were to determine whether predominant bowel habits and IBS symptom severity are related to pain sensitivity, colon motility, or smooth muscle tone.**

METHODS: **One hundred twenty-nine patients classified as IBS with diarrhea (IBS-D, N = 44), IBS with constipation (IBS-C, N = 29), mixed IBS (IBS-M, N = 45), and unspecified IBS (IBS-U, N = 11) based on stool consistency, and 30 healthy controls (HC) were studied. A manometric catheter containing a 600-mL capacity plastic bag was positioned in the descending colon. Pain threshold was assessed using a barostat. Motility was assessed for 10 min with the bag minimally inflated (individual operating pressure [IOP]), 10 min at 20 mmHg above the IOP, and for 15-min recovery following bag inflation. Motility was also recorded for 30 min following an 810-kcal meal.**

RESULTS: **Compared with HC, IBS patients had lower pain thresholds (medians 30 *vs* 40 mmHg, $P < 0.01$), but IBS subtypes were not different. IBS symptom severity was correlated with pain thresholds (rho = −0.36, $P < 0.001$). During distention, the motility index (MI) was significantly higher in IBS compared with HC (909 ± 73 *vs* 563 ± 78, $P < 0.01$). Average barostat bag volume at baseline was higher (muscle tone lower) in HC compared with IBS-D and IBS-M but not compared with IBS-C. The baseline MI and bag volume differed between IBS-D and IBS-C and correlated with symptoms of abdominal distention and dissatisfaction with bowel movements. Pain thresholds and MI during distention were uncorrelated.**

CONCLUSIONS: **Pain sensitivity and colon motility are independent factors contributing to IBS symptoms. Treatment may need to address both, and to be specific to predominant bowel habit.**

(Am J Gastroenterol 2008;103:2550–2561)

INTRODUCTION

There is no consensus on the pathophysiology of irritable bowel syndrome (IBS). In several studies, IBS patients had lower perception thresholds and increased sensations of discomfort to intraluminal distention in the sigmoid colon (1–3) and the rectum (4–6) (visceral hypersensitivity), or more exaggerated GI motility responses to experimental stress (7, 8), phasic intraluminal distention (9, 10), or eating (11, 12) (hyperreactive motility) compared with healthy controls (HC). However, there are only limited data on the extent to which visceral hypersensitivity and hyperreactive motility correlate with each other and influence clinical symptoms of abdominal pain and altered bowel habits (13).

Some reports suggest that patients with diarrhea-dominant IBS (IBS-D) have increased visceral sensitivity compared with those with constipation-dominant IBS (IBS-C) (14, 15), but others failed to find differences between subtypes (16, 17). Previous reports may be inconsistent because of a small number of subjects or other methodological differences. The guidelines for subclassifying IBS into IBS-C and IBS-D were recently revised (18). The former Rome II criteria (19) used multiple signs and symptoms to make this subclassification, which were complex and possibly unreliable, but the Rome III criteria simplified this classification by using only stool consistency (18). Most patients with IBS have a stool frequency within the normal range regardless of bowel pattern (20), but stool consistency (from watery to hard) reflects intestinal transit time (21). In this study, we used the Rome III criteria to identify subtypes of IBS.

Aims of this study were to: (a) compare IBS patients to HC with respect to pain sensitivity and tonic and

phasic colon motility, (b) determine whether IBS subtypes defined by usual stool consistency differ on these variables, (c) determine whether pain sensitivity is related to (*i.e.*, correlated with) phasic and tonic motility, and (d) determine whether IBS symptom severity is related to pain sensitivity, or tonic or phasic colon motility.

METHODS

Subjects

This was a prospective study. Subjects were recruited by advertisements or physician referrals and screened by telephone. The study population consisted of 136 patients who fulfilled Rome II criteria for IBS, received a physician diagnosis of IBS, and had current symptoms (abdominal pain or discomfort at least one-fourth of the time in the last 3 months). These subjects had no history of gastrointestinal surgery (other than appendectomy or cholecystectomy), inflammatory bowel disease, celiac disease, lactose malabsorption, heart disease, or diabetes mellitus, and they were not pregnant at the time of study.

Patients with IBS were classified by usual stool consistency into subtypes according to Rome III guidelines (18): IBS-D was defined as loose (mushy) or watery stool $\geq$25% and hard or lumpy stool <25% of bowel movements, and IBS-C was defined as hard or lumpy stool $\geq$25% and loose or watery stool <25% of bowel movements. IBS with mixed bowel habits (IBS-M) was defined as loose or watery stools $\geq$25% of the time plus hard or lumpy stools $\geq$25% of the time, and IBS with normal bowel habits (IBS-U, for unclassifiable) was defined by neither loose/watery nor hard/lumpy stools 25% or more of the time. The Rome III descriptions of stool consistencies were adapted from the Bristol Stool Scale, but the pictures of different stool forms were not provided to subjects.

The control population was recruited by advertisement and consisted of 33 subjects without any significant or recurring gastrointestinal symptoms. Exclusion criteria were average stool frequency of less than 3 per week or more than 3 per day, abdominal pain, or use of a laxative or antidiarrheal agent on more than two occasions over the prior year, history of alcohol or substance abuse, a psychiatric diagnosis, or any of the medical conditions listed above for the IBS patients. The study was approved by the Institutional Review Board of the University of North Carolina (UNC), and all subjects provided written informed consent.

Study Design

Subjects were admitted to the General Clinical Research Center at the University of North Carolina for a 24- to 30-h period. They were asked to fast for at least 4 h prior to reporting for admission. On the day of admission, a medical history, physical examination, and breath test for lactose intolerance and small intestinal bacterial overgrowth were completed. The Irritable Bowel Syndrome Severity Scale (22) (IBS-SS), the Brief Symptom Inventory-18 (23) (BSI-18), and other questionnaires were completed on a computer terminal during the breath test. A low-fiber meal was consumed at approximately 5:00 p.m. Day 1 ended with a bowel cleanout consisting of 1.5 oz of Fleet's phosphosoda consumed at 6:00 p.m. and repeated at 9:00 p.m.

QUESTIONNAIRES. The IBS-SS (22) is a validated scale for measuring the overall severity of IBS symptoms. It consists of five equally weighted questions. Subjects are asked to indicate for the past 10 days the average intensity of abdominal pain, the number of days with any abdominal pain, the average severity of abdominal distention, dissatisfaction with bowel habits, and the degree to which bowel symptoms interfered with their usual activities. Response to all except the pain frequency question are on a 1–100 numeric scale ("none" to "worst ever"), and the number of days of pain in the past 10 days is multiplied by 10 to arrive at a 0–100 score for this item. The five questions are added to arrive at a total score of 0–500.

The BSI-18 (23) is a validated questionnaire for measuring the degree of psychological distress over the past week. Subjects are asked how much they were bothered by each of 18 symptoms, and they respond on a 5-point ordinal scale from "not at all bothered" to "extremely." There are three subscales—anxiety, depression, and somatization—as well as a global severity index (GSI). Sum scores for each subscale and the GSI are converted to standardized scores where the mean for the healthy population is a score of 50 and each standard deviation from the mean is equal to 10 scale points; thus, a score of 60 is one standard deviation above the mean. These standardized scores adjust for sex differences in the reporting of psychological symptoms, so BSI-18 scores for men and women can be pooled together.

EQUIPMENT. The *barostat* is a computer-controlled pump (Distender II model, G&J Electronics, Willowdale, Ontario, Canada) used for testing sensory thresholds and smooth muscle tone in the lumen of the bowel. It inflates a plastic bag to a predefined pressure and holds this pressure constant for a fixed period of time by adding or subtracting air. Volumes and pressures are recorded 16 times per second and are displayed graphically in real time. The rate of inflation and deflation was 38 mL/s. Controlling the pump by means of a computer program made it possible to present complex sequences of distentions.

The *motility catheter* (Model C7-CB-0026, Mui Scientific, Mississauga, Ontario, Canada) is 5 mm in outside diameter. It consists of a bundle of smaller polyethylene tubes bonded together and includes a central lumen that accommodates a guide wire, two lumens that open inside the bag (one to inflate/deflate the bag and a second to monitor pressure inside the bag), plus four small catheters used to measure pressures 2.5 and 5 cm from the proximal and distal edges of the bag. A disposable, 10 cm long, 600 mL capacity polyethylene bag (Model CT-BP600R, Mui Scientific) was attached to the surface of the motility catheter and tied with surgical thread.

The *pneumohydraulic pump* (eight-channel hydraulic capillary infusion system, Arndorfer Inc, Greendale, WI) uses a tank of compressed air to force degassed sterile water from a reservoir through four capillary (very small diameter) catheters that are connected to four pressure transducers. These pressure transducers are also connected to the four small catheters in the motility catheter that open above and below the barostat bag. Water is perfused through the pressure transducers and the perfusion catheters at a rate of 0.37 mL/min. Because there is a continuous column of water connecting the pressure transducer to the openings on the outside of the motility catheter, pressure changes occurring at the openings are transmitted up the column of water to the pressure transducers. The outputs of these pressure transducers were continuously recorded (see below).

The *physiological recorder* used to record phasic and tonic motility changes above and below the balloon was a Synectics Polygram (Medtronic Inc., Minneapolis, MN). This instrument continuously recorded pressure changes above and below the bag and stored them in a digital file. A research nurse marked these recordings to indicate which experimental condition was in effect.

Colonic Sensory and Motility Testing

All physiological and sensory testing was performed on day 2 according to the protocol in Figure 1. On the morning of day 2 at approximately 8:00 a.m., the barostat catheter was placed in the descending colon for sensory and motility testing. First, a guide wire was inserted to the level of the splenic flexure using a flexible sigmoidoscope. The sigmoidoscope was then withdrawn and the motility catheter was guided over this wire. The guide wire was then withdrawn and barostat placement was confirmed by fluoroscopy. Following catheter placement, the subject rested for 90 min before testing began. No sedation was used during sigmoidoscopy. Subjects were not permitted to have food until the test meal (see Fig. 1).

SAMPLE DISTENTION AND DETERMINATION OF IOP. Subjects were instructed to give separate ratings of the intensity of pain and urgency to defecate experienced at the end of each distention, using a 6-point scale (0 = no sensation, 1 = weak, 2 = mild, 3 = moderate, 4 = strong, and 5 = intense). The scale was visible to subjects during the procedure. Sample distentions were then performed during which the barostat bag was inflated in a stepwise fashion by increasing bag pressure by 4 mmHg every 15 s until the subject reported moderate pain (rating of 3). The sample distentions served three purposes: (a) to insure that the barostat bag was unfolded, (b) to teach the subject how to use the rating scale to describe the intensity of colonic sensations, and (c) to decrease anticipatory anxiety. The barostat bag was then slowly inflated with 30 mL of air and the pressure was allowed to equilibrate for 3 min. The average bag pressure during the last 15 s defined the individual operating pressure (IOP) (24), which is the minimum pressure required to overcome mechanical forces and inflate the bag with 30 mL of air. All sensory and motility testing was done with the subject lying in a left-lateral position to minimize pressures because of the weight of overlying body tissues compressing the bowel.

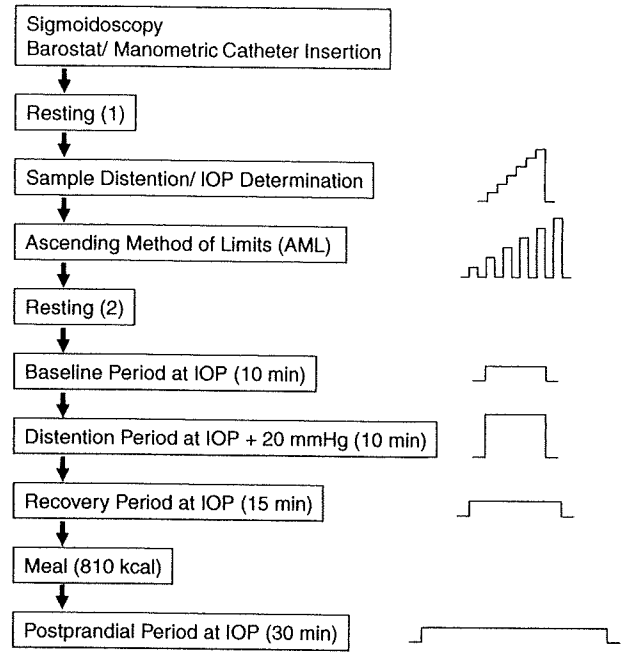

Figure 1. Study protocol. Graphs on right show sequence of pressure changes during each phase of testing. IOP (individual operating pressure) is the pressure required to overcome the weight of overlying tissue and minimally inflate the barostat bag.

ASCENDING METHOD OF LIMITS (AML). Pain thresholds in the colon were assessed using the AML (24). Phasic distentions were 30 s in duration and were separated by 30-s rest intervals. Distentions starting at the IOP and progressively increased in 2 mmHg steps until either the subject requested the research nurse to stop the protocol or 48 mmHg was reached. The pain threshold was defined as the amount of pressure above IOP at which the subject first reported moderate pain (absolute distending pressure *minus* the IOP). If the subject reached 48 mmHg without reporting moderate pain, then the pain threshold was defined as 50 mmHg *minus* the IOP. After measuring pain thresholds, there was a 15-min rest period. Individual pain thresholds are shown in Figure 2.

COLONIC PHASIC MOTILITY. Phasic contractions were measured from the perfusion ports above and below the bag under the following conditions: (a) during the fasting baseline for 10 min at the IOP, (b) during distention for 10 min at a pressure of IOP + 20 mmHg, (c) during a recovery period after intraluminal distention for 15 min at the IOP, and (d) following the meal for 30 min at the IOP. These tracings were visually screened to exclude artifact, defined as wave amplitudes less than 5 mmHg or with durations less than 6 s. The beginning

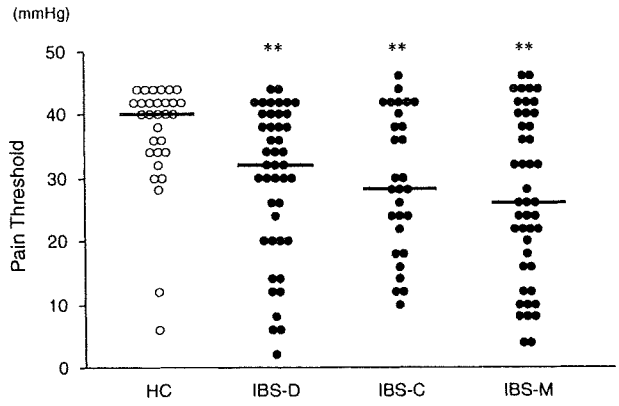

Figure 2. Pain threshold to intraluminal distention in the descending colon. Pain threshold in the descending colon was assessed using an electronic barostat by the ascending method of limit (AML). Each horizontal bar indicates the median value. The pain threshold was defined as the amount of pressure above IOP at which the subject first reported moderate pain (absolute distending pressure *minus* the IOP). If the subject reached 48 mmHg without reporting moderate pain, then the pain threshold was defined as 50 mmHg *minus* the IOP. HC = healthy controls (N = 30); IBS-D = IBS with diarrhea (N = 44); IBS-C = IBS with constipation (N = 29); IBS-M = mixed IBS (N = 45). $^{*}P < 0.05$, $^{**}P < 0.01$, *versus* controls.

and ending inflection points for each individual contraction were identified visually and the area under the curve was calculated using computer software (Polygram, Lower GI Edition, Version 5.06; Synectics Medical, now Medtronic, Inc., Minneapolis, MN). These areas were added together, then divided by recording time in seconds (excluding the time occupied by movement artifact), and multiplied by 100. The MI was the average of phasic contractions at four perfusion ports.

COLONIC TONIC MOTILITY. Average barostat bag volume in each period was recorded as a measure of smooth muscle tone (24). Muscle tone was measured during the fasting baseline, recovery period after intraluminal distention, and following the meal. The average volume required to maintain the barostat bag at a constant pressure was recorded. The average barostat bag volume in successive 5-min blocks constitutes an index of smooth muscle tone.

POSTPRANDIAL MOTILITY. The test meal was standardized and contained 810 kcals and 38 grams of fat. Subjects were asked to consume the meal within 10 min. Immediately after completing the meal, the patient returned to the prone position and bag pressure was maintained at the IOP for 30 min (the postprandial period). Phasic and tonic motility were recorded throughout this period.

Data Analysis

Phasic and tonic motility were assessed at baseline and in response to stimulation with intraluminal distention and meal ingestion. Because there were differences between groups at baseline, the response to stimulation had to be assessed after adjusting for baseline differences. To accomplish this, we expressed stimulated values as a percentage of baseline values. Absolute values are also presented in Table 2 to allow the reader to compare these two methods of data presentation. Statistical comparisons were performed on both the percent-of-baseline values and the absolute values.

Comparisons between groups were made using the Kruskal-Wallis test, followed by Mann-Whitney U-test. Correlations between variables were limited to the IBS patients, and employed the Spearman nonparametric correlation coefficient to account for nonnormal distributions of some variables. Multiple linear regression was used to determine which variables were most strongly associated with IBS symptom severity. In this analysis, dummy regression terms to code for usual stool consistency (hard or lumpy stool $\geq$25% and loose or watery stool $\geq$25%) were used (1 = yes, 0 = no). For all analyses, a P value of 0.05 without adjustment for multiple comparisons defined statistical significance.

Although this is the largest study to be reported comparing subgroups of IBS patients on physiological parameters, the subgroups were unequal in size (N = 45 for IBS-D, N = 29 for IBS-C, N = 45 for IBS-M, and N = 11 for IBS-U), and consequently the statistical power of between-group comparisons and correlations varied and could lead to spurious conclusions. Three steps were taken to avoid this: (a) no statistical comparisons were made to the IBS-U group and no correlations were reported for this subgroup because it was too small; (b) for other between-group comparisons, we identified the minimum Z-score for a Mann-Whitney U-test involving the smallest group (IBS-C) that was significant at $P < 0.05$ and interpreted other comparisons as statistically significant only if they exceeded this critical value; and (c) similarly, for Spearman nonparametric correlations, we identified the smallest correlation of a group of size N = 29 that was significant at $P < 0.05$ and interpreted other correlations as statistically significant only if they exceeded this critical value.

RESULTS

Eligible Subjects

One hundred twenty-nine IBS patients (20 men; mean age 35.8 yr) and 30 healthy control subjects (8 men; 37.2 yr) underwent both colonic sensory and motility tests. Seven additional IBS patients were enrolled but did not undergo colonic sensory and motility testing: three refused flexible sigmoidscopy, two began but could not tolerate completion of unsedated sigmoidscopy, one had an extremely elevated blood pressure, and one had colonic inflammation detected on sigmoidscopy. Three additional control subjects were similarly screened but excluded: one did not tolerate the flexible sigmoidscopy and two had exclusionary medical conditions that were detected during the study (lactose intolerance in one and prior colonic surgery in the other).

Table 1. Demographics, IBS Symptom Severity, and Psychological Distress Scales

	Controls	IBS total	IBS-D	IBS-C	IBS-M	IBS-U[¶]
Number	30	129	44	29	45	11
Women n (%)	22 (73)	109 (84)	34 (77)	26 (90)	38 (84)	11 (100)
Age (yr)	37.2 ± 2.2	35.8 ± 1.1	36.6 ± 2.0	34.9 ± 2.0	35.1 ± 1.9	38.4 ± 3.5
Race						
White	13	90	31	16	37	6
Non-white	14	36	12	12	7	5
Unknown	3	3	1	1	1	0
IBS-SS						
Overall	27.9 ± 9.8	273.2 ± 8.1[†]	255.8 ± 15.1[†]	281.1 ± 16.5[†]	282.2 ± 13.6[†]	287.9 ± 13.2
Pain severity	4.7 ± 2.4	47.0 ± 2.2[†]	43.3 ± 3.8[†]	45.5 ± 4.5[†]	48.2 ± 3.9[†]	64.4 ± 5.6
Pain frequency	4.5 ± 2.3	47.2 ± 2.1[†]	43.4 ± 3.6[†]	46.6 ± 4.5[†]	48.9 ± 3.7[†]	58.9 ± 5.1
Distention	3.3 ± 1.5	44.8 ± 2.6[†]	38.5 ± 4.7[†]	51.4 ± 5.3[†]	48.4 ± 4.1[†]	35.7 ± 8.8
Bowel dissatisfaction	18.0 ± 5.8	77.6 ± 2.2[†]	72.9 ± 4.3[†]	80.7 ± 4.0[†]	80.7 ± 3.2[†]	75.0 ± 9.1
QOL	2.7 ± 1.9	56.4 ± 2.6[†]	57.2 ± 4.6[†]	56.9 ± 5.3[†]	55.9 ± 4.1[†]	53.9 ± 11.0
BSI-18						
Global scale	42.3 ± 1.5	52.4 ± 0.8[†]	53.4 ± 1.5[†]	51.6 ± 1.6[†]	52.5 ± 1.2[†]	49.8 ± 3.6
Somatization	44.8 ± 1.2	54.1 ± 0.7[†]	55.5 ± 1.1[†]	52.8 ± 1.6[†]	53.9 ± 1.0[†]	52.9 ± 3.4
Depression	46.0 ± 1.5	51.0 ± 1.0[*]	52.6 ± 1.9[†]	52.0 ± 1.8[*]	49.4 ± 1.6	49.0 ± 5.1
Anxiety	43.3 ± 1.2	51.1 ± 0.8[†]	51.7 ± 1.4[†]	50.6 ± 1.7[†]	51.8 ± 1.4[†]	45.8 ± 2.6

[¶]No statistical comparisons were made to the IBS-U group because of a small sample size.
Data were shown as mean ± SEM.
[*]$P < 0.05$; [†]$P < 0.01$, compared with controls, Mann-Whitney U-test.
IBS-SS = IBS severity scale; BSI-18 = brief symptom index 18.

Two of 129 eligible patients did not complete the postprandial assessment because of unpleasant symptoms experienced during the test meal. One patient did not complete only the postprandial tonic motility assessment because of equipment failure. Two patients and one control subject did not report symptom severity on the IBS-SS. No serious adverse events were observed.

Table 1 shows demographic characteristics of the sample. There were no differences between HC and IBS patients in gender, age, or race/ethnicity.

IBS Symptom Severity and Psychological Distress

Scores on the IBS-SS and the BSI-18 are shown in Table 1. IBS patients scored significantly higher than HC on the IBS-SS total score and all subscales of the IBS-SS. Figure A1 in the Appendix shows IBS-SS scores for all subjects separated into groups. This figure demonstrates that the IBS-SS scores were normally distributed within the IBS subgroups and that there was no tendency for the subtypes of IBS to differ from each other. On the BSI-18, IBS patients also scored significantly higher than HC on all subscales and on the global symptom index. However, there were no significant differences among the IBS subtypes.

Pain Sensitivity

IBS patients had significantly lower thresholds for pain on the barostat test compared with HC (Table 2). Figure 2 shows the distribution of pain thresholds for each group. All IBS subtypes had significantly lower pain thresholds than HC, and for 57% of IBS patients, pain thresholds were below

Table 2. Sensory Thresholds and Colonic Motility Responses in Subtypes of IBS

	Controls (N = 30)	IBS Total (N = 129)	IBS-D (N = 44)	IBS-C (N = 29)	IBS-M (N = 45)	IBS-U[¶] (N = 11)
Pain threshold (mmHg)	40 [6–44]	30 [2–46][†]	32 [2–44][†]	28 [10–46][†]	26 [4–46][†]	36 [6–42]
Motility Index						
Baseline	280 ± 33	311 ± 19	370 ± 37	271 ± 35[§]	290 ± 32	263 ± 40
Distention	563 ± 78[‖]	909 ± 73[†,‖]	840 ± 127[*,‖]	1,001 ± 208[‖]	914 ± 99[†,‖]	927 ± 162
Recovery	302 ± 30	430 ± 31[‖]	531 ± 61[*,‖]	422 ± 65[†]	372 ± 45[†]	288 ± 40
Postmeal	429 + 49[‖]	481 + 28[‖]	542 ± 60[†]	422 ± 47[‖]	477 ± 45[§,‖]	410 ± 61
IOP (mmHg)	9.1 ± 0.6	9.3 ± 0.3	9.8 ± 0.6	9.4 ± 0.6	8.8 ± 0.5	8.4 ± 0.8
Tone (mL)						
Baseline	54.8 ± 7.9	40.1 ± 2.8[*]	32.5 ± 3.1[*]	48.7 ± 6.9[§]	38.3 ± 4.5[*]	55.3 ± 14.5
Recovery	54.2 ± 7.9	38.6 ± 2.8[*]	34.5 ± 4.0[*]	42.8 ± 5.8	36.6 ± 4.7[*]	52.2 ± 14.6
Postmeal	21.1 ± 2.5[‖]	18.8 ± 1.2[‖]	18.6 ± 1.6[‖]	20.5 ± 3.3[‖]	17.6 ± 2.0[‖]	19.6 ± 5.0

[¶]No statistical comparisons were made to the IBS-U group because of a small sample size.
Sensory thresholds are shown as medians with range and motility data are shown as means ± SEM.
[*]$P < 0.05$; [†]$P < 0.01$, compared with controls; [§]$P < 0.05$, compared with IBS-D; [‡]$P < 0.05$; [‖]$P < 0.01$, compared with each baseline, Mann-Whitney U-test.

the 95% confidence interval for controls (34 mmHg). There were no significant differences in pain thresholds between the subtypes of IBS.

Phasic Colon Motility

BASELINE. When tested under baseline conditions (fasting, no intraluminal distention), the MI (phasic contractions) was no different in the total IBS patient group *versus* HC (Table 2). However, the IBS-D group showed significantly more phasic contractions than IBS-C.

RESPONSE TO INTRALUMINAL DISTENTION. As shown in Table 2, both HC and IBS groups showed a significant increase in MI during intraluminal distention. The magnitude of this increase was greater in the IBS patients compared with HC. The magnitude of the increase in MI from baseline to distention was significantly greater in the IBS-C and IBS-M groups compared with HC ($P < 0.05$), but the subtypes of IBS did not differ from each other in magnitude of increase in phasic motility from baseline. Figure A2 in the Appendix shows responses to distention as a percentage of baseline values. Statistical analysis of these baseline-adjusted values showed the same significant comparisons as did analysis of the absolute values.

During the recovery period following intraluminal distention, the MI decreased and was not significantly different from baseline for either HC or IBS patients (all subtypes combined). When the IBS subtypes were compared with each other during recovery from distention, there were no significant differences between the subtypes.

RESPONSE TO EATING. As shown in Table 2, both HC and IBS showed significant increases in MI following the meal, but the magnitude of this increase was similar in IBS *versus* HC. There was no significant difference between IBS subtypes in the magnitude of the meal-stimulated increase in phasic contractions. Figure A2 in the Appendix shows responses to the meal as a percent of baseline values. Statistical analysis of these baseline-adjusted values also failed to show differences between HC *versus* IBS or between IBS subgroups.

Smooth Muscle Tone Measured by Barostat Bag Volume

BASELINE. When tested in the fasting state and without intraluminal distention, barostat bag volumes were smaller (*i.e.*, smooth muscle tone was greater) in IBS compared with HC (Table 2). Comparison of IBS subtypes showed that the IBS-D subgroup had significantly lower bag volumes than the IBS-C group. Because IBS-M patients, like IBS-D patients, have loose or watery stools at least 25% of the time, we performed a *post hoc* comparison of the IBS-D and IBS-M groups combined *versus* the IBS-C and IBS-U groups combined and found that this was significant; as a group, patients who reported $\geq$25% of bowel movements as loose or watery had lower barostat bag volumes (35.4 $\pm$ 2.7 mL) than IBS patients whose bowel movements were rarely loose or watery (50.5 $\pm$ 6.3 mL, $P < 0.05$).

RECOVERY PERIOD FOLLOWING DISTENTION. Muscle tone could not be measured during distention because barostat bag volumes during distention reflect compliance rather than tone. Barostat bag volumes during recovery from distention were approximately the same as during baseline and again showed lower bag volumes in the total IBS sample and in the IBS-D and IBS-M subgroups compared with the HC group (Table 2).

RESPONSE TO EATING. As shown in Table 2, both HC and IBS exhibited a statistically significant and profound decrease in bag volumes (*i.e.*, an increase in smooth muscle tone) following the meal. The magnitude of this change in bag volume was not significantly different between IBS and HC. When the IBS subtypes were compared with each other, there was no difference in muscle tone between the subtypes (Table 2). Figure A3 in the Appendix shows meal-related changes in bag volume as a percentage of baseline values. Statistical analysis of these baseline-adjusted values also failed to show differences between IBS and HC or differences between IBS subtypes.

Relationship Between Motility and Sensory Thresholds

Figure 3 shows the relationship between the MI and the threshold for pain perception. Dotted vertical and horizontal lines show where the 95% confidence interval for HC lies on each of these dimensions. The overall correlation between motility during distention and pain sensory threshold in IBS patients was rho = -0.06 ($P > 0.1$, see Fig. 3), suggesting that these are independent dimensions.

Relationship of IBS Symptom Severity to Visceral Perception, Colonic Motility, and Psychological Symptoms

When all subtypes of IBS were pooled together, the pain threshold was significantly correlated with overall symptom severity (rho = -0.36, $P < 0.001$), intensity of abdominal pain (rho = -0.34, $P < 0.001$), frequency of abdominal pain (rho = -0.32, $P < 0.001$), and severity of abdominal distention (rho = -0.31, $P < 0.001$). Neither phasic motility nor smooth muscle tone was significantly correlated with overall symptom severity or with individual symptoms on the IBS-SS. However, because there were differences in motility between IBS-D and IBS-C (as shown in Table 2), it was possible that associations between motility and clinical symptoms were obscured by pooling all IBS subtypes together. Therefore, the correlations between motility parameters and key clinical symptoms (frequency of clinical pain, intensity of abdominal distention, and dissatisfaction with bowel habits) were computed for each IBS subtype separately. These data are summarized below.

ABDOMINAL PAIN. Clinical pain frequency was significantly correlated with pain threshold in IBS-D (rho = -0.33,

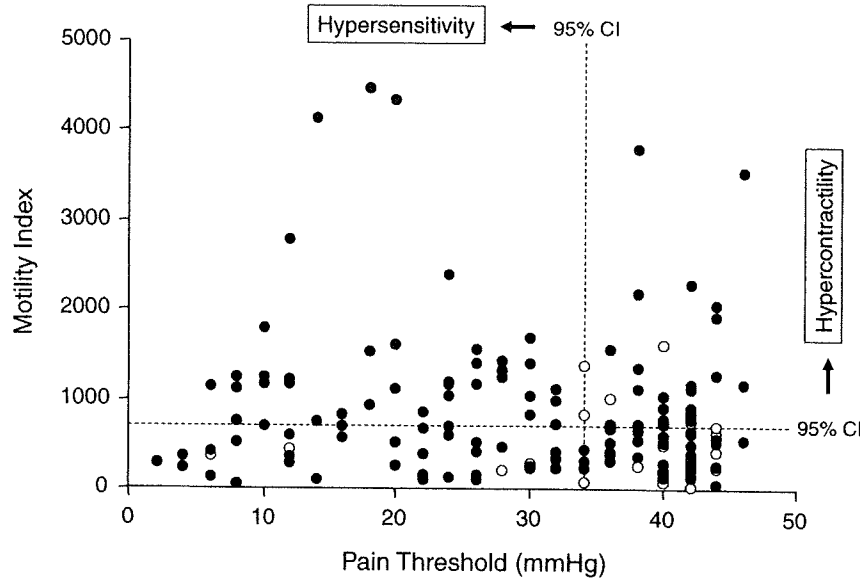

Figure 3. Relationship between colonic motility during distention period and pain threshold. No significant relationship was observed between colonic motility during distention period and visceral sensitivity in IBS patients (N = 129; closed circles) or healthy subjects (N = 30; open circles). Dashed lines show the 95% confidence intervals (CI): 49% of IBS patients showed contractile activity above the CI for controls in response to intraluminal distention, and 57% of patients had pain thresholds below the CI for controls. Of these patients, 31% showed both visceral hypercontractivity and pain hypersensitivity.

$P < 0.05$) and this correlation was even stronger in IBS-M (rho = -0.50, $P < 0.001$). However, there was no correlation between pain threshold and clinical pain frequency in IBS-C (rho = -0.13, NS).

ABDOMINAL DISTENTION. The motility index was negatively correlated with severity of abdominal distention in IBS-C (rho = -0.39, $P < 0.05$), but the motility index was unrelated to distention severity in IBS-D and IBS-M. The negative correlation indicates that as the amount of phasic contractions increased in IBS-C, the severity of distention decreased.

DISSATISFACTION WITH BOWEL HABITS. The symptom of dissatisfaction with bowel habits correlated negatively (rho = -0.40, $P < 0.01$) with postprandial smooth muscle tone in IBS-D (*i.e.*, smaller bag volumes because of greater smooth muscle tone were associated with greater dissatisfaction with bowel habits). Among IBS-M and IBS-C, there was no association with muscle tone.

PSYCHOLOGICAL SYMPTOMS. When all IBS patients were analyzed together as one group, somatization (the tendency to notice and report somatic sensations possibly indicative of disease) was significantly correlated with overall IBS symptom severity (rho = 0.30, $P < 0.01$), and with the IBS-SS subscales for pain frequency (rho = 0.23, $P < 0.05$) and abdominal distention (rho = 0.21, $P < 0.05$). Anxiety and depression were not significantly related to bowel symptoms. When the subtypes of IBS were analyzed separately, the association between somatization and bowel symptom severity was found to be significant only for the IBS-M subtype: (rho = 0.36 for pain frequency, rho = 0.30 for abdominal distention, and rho = -0.30 for dissatisfaction with bowel movements; all significant at $P < 0.05$). Depression was significantly correlated with dissatisfaction with bowel movements, but only in the IBS-C group.

Multiple linear regression (Table 3) was used to determine whether pain threshold, phasic motility, tonic motility, BSI psychological scales for somatization, depression and anxiety, and dominant stool consistency make independent contributions to IBS symptom severity after adjusting for the intercorrelations among these independent measures. Separate regression models were run for overall IBS symptom severity and the component clinical symptoms of pain intensity, pain frequency, abdominal distention severity, and dissatisfaction with bowel movements. The regression analyses showed that a significant amount of variance in IBS symptom severity was explained by these models for all dependent variables except dissatisfaction with bowel movements; the amount of variance explained (R^2) ranged from 0.22 to 0.26 for the four significant models. Pain threshold was a significant independent predictor ($P < 0.001$) in all of these models except dissatisfaction with bowel movements, and motility index during recovery was a significant predictor for pain intensity ($\beta = 0.27$, $P < 0.05$) and abdominal distention ($\beta = -0.29$, $P < 0.05$). Somatization was a significant independent predictor for overall symptom severity ($\beta = 0.23$, $P < 0.05$) and abdominal distention ($\beta = 0.24$, $P < 0.05$). For abdominal distention, having hard or lumpy stools at least 25% of the time was also a significant predictor ($\beta = 0.20$,

Table 3. Multiple Linear Regression Analyses for IBS Symptoms Severity in Patients With IBS (N = 129)

	IBS-SS Overall	Pain Intensity	Pain Frequency	Distention Severity	Bowel Dissatisfaction
R^2	0.26†	0.23†	0.22*	0.26†	0.07
Covariates (β)					
Pain threshold	−0.36‡	−0.35‡	−0.33‡	−0.35‡	0.06
Baseline MI	−0.01	−0.08	−0.12	0.18	0.08
Distention MI	0.00	0.02	0.05	−0.10	−0.03
Recovery MI	0.01	0.27*	0.15	−0.29*	0.01
Postmeal MI	−0.08	−0.18	−0.11	0.05	−0.02
Baseline tone	0.10	0.11	0.17	0.01	0.10
Recovery tone	−0.09	−0.02	−0.15	−0.12	−0.07
Postmeal tone	0.06	0.01	0.08	−0.04	−0.14
BSI somatization	0.23*	0.12	0.13	0.24*	−0.07
BSI depression	0.11	−0.04	0.03	0.03	−0.06
BSI anxiety	−0.08	−0.03	−0.06	−0.01	0.00
Hard/lumpy stools ≥25%	0.08	−0.02	0.01	0.20*	−0.13
Loose/watery stools ≥25%	−0.04	−0.07	−0.04	−0.07	−0.02

The model included the following variables: Pain threshold, phasic and tonic motility, T-scores of BSI psychological scales for somatization, depression, and anxiety, hard or lumpy stools ≥25% (yes = 1, no = 0) and loose or watery stools ≥25% (yes = 1, no = 0).
*$P < 0.05$; †$P < 0.01$; ‡$P < 0.001$.
IBS-SS = IBS severity scale; MI = motility index; BSI = brief symptom index.

$P < 0.05$). Smooth muscle tone was not a significant predictor in any of the models.

DISCUSSION

This large, carefully conducted study yielded three important and novel findings: First, we confirmed that visceral pain hypersensitivity is associated with (and likely contributes to) greater severity of IBS clinical symptoms, especially the frequency and the typical intensity of abdominal pain. This association was not explained by psychological influences on symptom reporting. Second, when IBS patients were divided into subtypes based on the frequency of loose or watery stools and/or the frequency of hard or lumpy stools, we found significant differences between the subtypes in both phasic and tonic motility of the descending colon (differences in phasic motility have been previously described but differences in muscle tone have not). Third, the relationship between clinical symptoms and motility differed depending on predominant bowel habits. Thus, both pain thresholds and motility have an impact on the severity of specific IBS symptoms: pain thresholds show their strongest associations with clinical pain while motility is more strongly associated with abdominal distention and dissatisfaction with bowel movements.

Hypersensitivity for Visceral Pain

Our data are consistent with a large body of research, which shows that IBS patients exhibit hypersensitivity to intraluminal distention: 57% of our IBS patients had pain thresholds that were below the normal range, that is, below the confidence interval for pain thresholds in healthy controls (Fig. 2). A strength of this study is that sensory thresholds were studied in the descending colon rather than the rectum; most previous studies of visceral perception have tested pain sensitivity in the rectum even though it is assumed that the symptoms of IBS originate predominantly from the colon or small intestine.

Pain thresholds were significantly correlated with the overall severity of IBS symptoms. Individual symptoms that correlated with pain threshold were clinical pain intensity, pain frequency, and the severity of distention. Somatization (the psychological tendency to notice and report symptoms) was also correlated with clinical pain, abdominal distention, and overall symptom severity. However, the association between pain threshold and clinical symptoms remained significant after adjusting for the correlation of clinical symptoms with somatization, anxiety, and depression (Table 3).

We observed no significant differences in pain thresholds between IBS subtypes defined by Rome III criteria. Our findings are in agreement with previous barostat studies in the *rectum* that showed no significant differences between IBS-D and IBS-C for pain thresholds (15, 25), although previous studies showed that *rectal* urge thresholds were lower in IBS-D patients compared with IBS-C patients (15, 25). Earlier studies using volume distentions, instead of pressure or tension-scaled distentions, reported lower pain thresholds in IBS-D compared with IBS-C, which is consistent with our observation that IBS-D patients have increased muscle tone compared with IBS-C (Table 2). These data extend earlier studies by showing that in the colon as well as the rectum, pressure-scaled pain thresholds are similar in IBS-D *versus* IBS-C.

Phasic Motility

Previous reports have been inconsistent as to whether IBS patients have more phasic contractions than HC under baseline conditions (*i.e.*, fasting and without stimulation by distention, stress, or exogenous hormones): there have been reports that IBS patients show more baseline motility (26, 27), less motility (28), and about the same amount (9, 10) compared

with HC. We found no difference when comparing HC to all IBS patients combined. However, the IBS-D group showed significantly more baseline contractile activity than IBS-C. We believe our results are generalizable because our study was relatively large (N = 129 IBS patients and 30 HC) and we visually identified each phasic contraction and calculated its area under the curve rather than relying on the less precise method of allowing a computer program to estimate the MI by integrating the area of all activity above an arbitrary baseline.

Sustained intraluminal distention simulates a frequently occurring physiological stimulus to the colon, namely distention of the colon by fecal material or gas. This stimulus evokes an increase in phasic motility in both HC and IBS patients, but the increase is significantly greater in IBS patients. This exaggerated response to intraluminal distention has been termed "hyperreactivity" (29), and our data suggest that it is characteristic of all IBS patients rather than being limited to one subtype. We first reported that IBS is characterized by this exaggerated response to intraluminal distention in 1980 (10) and other laboratories have replicated this observation (9). The response to distention is reversible—MI returns to baseline when the distending stimulus is removed (Table 2)—and in other studies we have shown that it is reproducible on a second occasion of testing (10). These characteristics make the response to intraluminal distention an attractive probe of motility for investigations of IBS. However, there is overlap between IBS and HC, rendering MI of limited value as a diagnostic marker for IBS.

Eating also stimulates an increase in the MI in both HC and IBS, as others have also shown (11). We did not find that the magnitude of the meal stimulation was significantly greater in IBS patients as a group compared with HC. There were no differences in postprandial stimulation of MI between IBS subgroups.

To summarize our findings with respect to phasic contractions of the colon: (a) phasic contractions increase in reaction both to intraluminal distention and eating; (b) compared with healthy controls, IBS patients show an exaggerated response to intraluminal distention but a similar response to eating; and (c) IBS-D patients have more baseline phasic motility than IBS-C, but the differences are modest and there is overlap.

Barostat Bag Volumes

Average barostat bag volumes measured at the IOP provide an indirect measure of smooth muscle tone. As previously reported (30), IBS patients have lower bag volumes than HC, indicating that IBS is associated with increased smooth muscle tone. Our data confirm this observation and extend it by showing that elevated smooth muscle tone is limited to patients with loose or watery stools at least 25% of the time. Patients with IBS-D had significantly lower bag volumes than patients with IBS-C (Table 2).

As previously reported (27, 31), barostat bag volumes decrease substantially following a meal (Table 2), indicating an increase in smooth muscle tone in the descending colon. However, the magnitude of the increase in smooth muscle tone is similar in IBS *versus* HC, and it does not distinguish patients with IBS-D from those with IBS-C. This increase in smooth muscle tone, along with the increase in phasic motility following a meal, are believed to be part of the physiological mechanism resulting in a tendency for flatus and defecation to occur shortly after a meal.

We anticipated that phasic motility and smooth muscle tone would be related to IBS symptoms, especially to dissatisfaction with bowel habits. No associations between motility and symptoms were seen when all IBS patients were considered together. However, when IBS subtypes defined by Rome III criteria were analyzed separately, we found significant but contrasting associations: (a) bowel dissatisfaction was significantly correlated with smooth muscle tone in the IBS-D group and (b) abdominal distention was negatively correlated with phasic motility in IBS-C (decreased muscle contraction associated with increased distention severity) but not IBS-D. In general, the associations between motility parameters and clinical symptoms were weaker than the associations between pain threshold and clinical symptoms, and some of these univariate associations could not be confirmed by regression analysis. Other variables such as somatization are also significant predictors of clinical symptoms in IBS.

Relationship Between Pain Sensitivity and Motility

IBS patients demonstrate both hypersensitivity and hyperreactive motility in comparison to healthy controls. These appear to be independent pathophysiological mechanisms because (a) there is no correlation between them and (b) they show different relationships to the symptoms of IBS. Pain hypersensitivity is associated with more severe clinical pain and distention but is unrelated to dissatisfaction with bowel movements, and pain thresholds do not differ between IBS-D and IBS-C. Phasic motility and smooth muscle tone, on the other hand, are greater in IBS-D than they are in IBS-C and may play a role in regulating usual or predominant bowel habits. We did not, however, find that hyperreactive motility could reliably differentiate between patients with IBS-D and those with IBS-C. The apparent independence of pain hypersensitivity and motility suggests that different etiologies—genetic, inflammatory, psychosocial, or other factors— are likely to be found for motility hyperreactivity and pain sensitivity, and different treatments or management strategies may be required.

Study Limitations

It is possible that the invasive nature of the test protocol, which required unsedated sigmoidoscopy to place the motility catheter and led subjects to anticipate pain and/or anxiety, may have biased recruitment. Consistent with this possibility, the average age of the IBS sample was 35.8 yr, which is younger than average for the IBS patients we have studied in other settings (32). Second, the prevalence of pain hypersensitivity may have been underestimated because five IBS

patients and one HC were unable or unwilling to undergo unsedated flexible sigmoidoscopy after volunteering. Both of these study limitations could have led to an underrepresentation of IBS patients with the greatest pain sensitivity, but this would not affect the conclusions that pain sensitivity and motility reactivity are independent pathophysiological mechanisms for IBS and that pain sensitivity is the more important determinant of clinical symptoms. A third limitation is that the motility parameters tested were restricted to phasic and tonic motility in the descending colon and did not include small bowel motility (33) or high-amplitude propagating contractions (34, 35). Thus, we may have overlooked motility patterns that show a stronger association with IBS symptom severity or altered bowel habits.

Significance

This study shows that both pain thresholds and motility have an impact on the severity of specific IBS symptoms: pain thresholds show their strongest associations with clinical pain while motility is more strongly associated with abdominal distention and dissatisfaction with bowel movements. Our data further suggest that pain sensitivity and motility are independent physiological mechanisms for the symptoms of IBS. The implication of these findings for clinical practice is that treatments may have to be selected based on the patient's predominant bowel habit in order to maximize clinical benefit. Furthermore, because most drugs currently approved for the treatment of IBS have a greater impact on motility than on pain, clinicians may want to supplement current drug treatments for IBS with a pain management strategy. The implication for pharmaceutical companies is that it may be advantageous to target pain sensitivity in future drug development programs.

STUDY HIGHLIGHTS

What Is Current Knowledge

- Patients with irritable bowel syndrome (IBS) show visceral hypersensitivity or hyperreactive motility in the sigmoid colon and the rectum.

What Is New Here

- Visceral pain sensitivity in the descending colon is associated with greater severity of IBS clinical symptoms, especially abdominal pain.
- Phasic and tonic colon motility are related to predominant bowel habits and to the clinical symptoms of abdominal distention and dissatisfaction with bowel movements.
- Visceral hypersensitivity and motility are independent physiological mechanisms for the symptoms of IBS.

APPENDIX

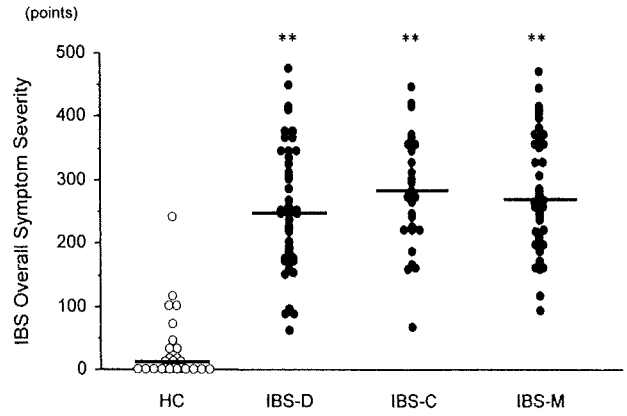

Figure A1. IBS symptom severity scale (IBS-SS) in subtypes of IBS and healthy controls. IBS-SS total score for each subject is shown. Each horizontal bar indicates the median value. HC = healthy controls (N = 30); IBS-D = IBS with diarrhea (N = 44); IBS-C = IBS with constipation (N = 29); IBS-M = mixed IBS (N = 45). $^{**}P < 0.01$, *versus* controls.

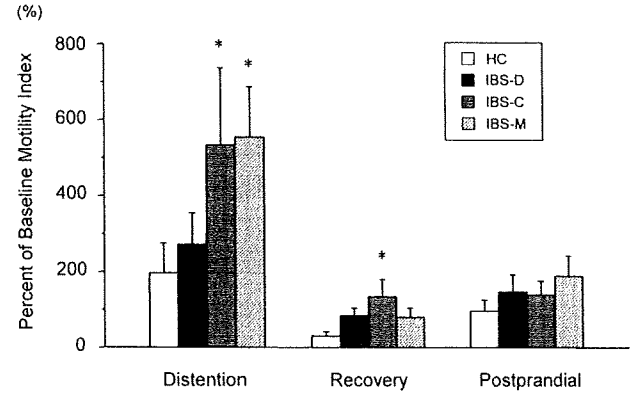

Figure A2. Changes in motility index during each stimulus period in subtypes of IBS and healthy controls. Distention, the MI during recovery and postprandial periods, is expressed as a percentage of the baseline MI for the subgroup to adjust for any baseline differences. HC = healthy controls (N = 30); IBS-D = IBS with diarrhea (N = 44); IBS-C = IBS with constipation (N = 29); IBS-M = mixed IBS (N = 45). Data were expressed as mean + SEM. $^{*}P < 0.05$ *versus* controls in same phase of testing. During distention and postprandial periods, all groups are significantly ($P < 0.05$) greater than baseline.

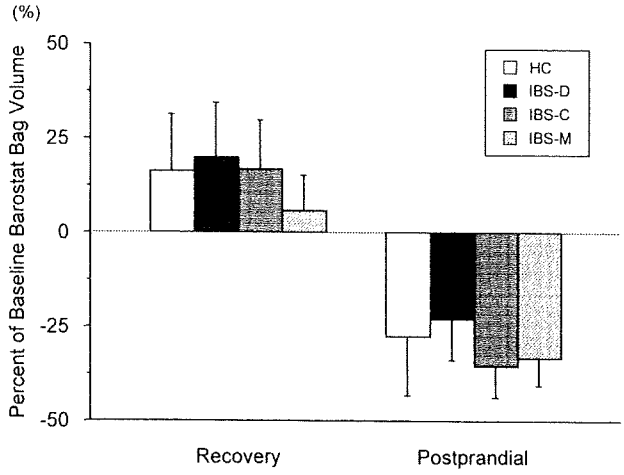

Figure A3. Changes in colonic muscle tone during each stimulus period in subtypes of IBS and healthy controls. The colonic muscle tone was measured as mean bag volume. For the recovery and postprandial periods, each bar shows percentage of baseline value for the subgroup. HC = healthy controls; IBS-D = IBS with diarrhea; IBS-C = IBS with constipation; IBS-M = mixed IBS. Data were expressed as mean ± SEM. Groups are not significantly different from each other within conditions, but postprandial values are significantly ($P < 0.05$) lower than baseline for all groups.

Reprint requests and correspondence: Motoyori Kanazawa, M.D., Ph.D., Department of Behavioral Medicine, Tohoku University Graduate School of Medicine, 2-1 Seiryo, Aoba, Sendai 980-8575, Japan.

Received September 5, 2007; accepted May 26, 2008

REFERENCES

1. Ritchie J. Pain from distension of the pelvic colon by inflating a balloon in the irritable colon syndrome. Gut 1973;14:125–2.
2. Whitehead WE, Holtkotter B, Enck P, et al. Tolerance for rectosigmoid distention in irritable bowel syndrome. Gastroenterology 1990;98:1187–92.
3. Dorn SD, Palsson OS, Thiwan SIM, et al. Colonic pain sensitivity in irritable bowel syndrome is the result of an increased tendency to report pain rather than increased neurosensory sensitivity. Gut 2007;56:1202–9.
4. Mertz H, Naliboff B, Munakata J, et al. Altered rectal perception is a biological marker of patients with irritable bowel syndrome. Gastroenterology 1995;109:40–52.
5. Bouin M, Plourde V, Boivin M, et al. Rectal distention testing in patients with irritable bowel syndrome: Sensitivity, specificity, and predictive values of pain sensory thresholds. Gastroenterology 2002;122:1771–7.
6. Distrutti E, Salvioli B, Azpiroz F, et al. Rectal function and bowel habit in irritable bowel syndrome. Am J Gastroenterol 2004;99:131–7.
7. Fukudo S, Suzuki J. Colonic motility, autonomic function, and gastrointestinal hormones under psychological stress on irritable bowel syndrome. Tohoku J Exp Med 1987;151:373–85.
8. Welgan P, Meshkinpour H, Hoehler F. The effect of stress on colon motor and electrical activity in irritable bowel syndrome. Psychosom Med 1985;47:139–49.
9. Fukudo S, Kanazawa M, Kano M, et al. Exaggerated motility of the descending colon with repetitive distention of the sigmoid colon in patients with irritable bowel syndrome. J Gastroenterol 2002;37(Suppl 14):145–50.
10. Whitehead WE, Engel BT, Schuster MM. Irritable bowel syndrome – physiological and psychological differences between diarrhea-predominant and constipation-predominant patients. Dig Dis Sci 1980;25:404–13.
11. Sullivan MA, Cohen S, Snape WJ Jr. Colonic myoelectrical activity in irritable-bowel syndrome. Effect of eating and anticholinergics. N Engl J Med 1978;298:878–3.
12. Di Stefano M, Miceli E, Missanelli A, et al. Meal induced rectosigmoid tone modification: A low caloric meal accurately separates functional and organic gastrointestinal disease patients. Gut 2006;55:1409–14.
13. Drossman DA, Whitehead WE, Toner BB, et al. What determines severity among patients with painful functional bowel disorders? Am J Gastroenterol 2000;95:974–80.
14. Prior A, Maxton DG, Whorwell PJ. Anorectal manometry in irritable bowel syndrome – differences between diarrhea and constipation predominant subjects. Gut 1990;31:458–62.
15. Steens J, Van Der Schaar PJ, Penning C, et al. Compliance, tone and sensitivity of the rectum in different subtypes of irritable bowel syndrome. Neurogastroenterol Motil 2002;14:241–7.
16. Simren M, Abrahamsson H, Bjornsson ES. An exaggerated sensory component of the gastrocolonic response in patients with irritable bowel syndrome. Gut 2001;48:20–7.
17. Caldarella MP, Milano A, Laterza F, et al. Visceral sensitivity and symptoms in patients with constipation- or diarrhea-predominant irritable bowel syndrome (IBS): Effect of a low-fat intraduodenal infusion. Am J Gastroenterol 2005;100:383–9.
18. Longstreth GF, Thompson WG, Houghton LA, et al. Functional bowel disorders. In: Drossman DA, Corazziari E, Delvaux M, et al., eds. Rome III: The functional gastrointestinal disorders, 3rd Ed. McLean, VA: Degnon Associates, 2006:487–555.
19. Thompson WG, Longstreth G, Drossman DA, et al. Functional bowel disorders and functional abdominal pain. In: Drossman DA, Corazziari E, Talley NJ, et al, eds, Rome II: The functional gastrointestinal disorders, 2nd Ed. McLean, VA: Degnon Associates, 2000:351–432.
20. Mearin F, Balboa A, Badia X, et al. Irritable bowel syndrome subtypes according to bowel habit: Revisiting the alternating subtype. Eur J Gastroenterol Hepatol 2003;15:165–72.
21. Lewis SJ, Heaton KW. Stool form scale as a useful guide to intestinal transit time. Scand J Gastroenterol 1997;32:920–4.
22. Francis CY, Morris J, Whorwell PJ. The irritable bowel severity scoring system: A simple method of monitoring irritable bowel syndrome and its progress. Aliment Pharmacol Ther 1997;11:395–402.
23. Derogatis LR. BSI 18 Brief symptom inventory 18: Administration, scoring, and procedures manual. NCS Pearson, Inc, 2000.
24. Whitehead WE, Delvaux M, Azpiroz F. Standardization of barostat procedures for testing smooth muscle tone and sensory thresholds in the gastrointestinal tract. Dig Dis Sci 1997;42:223–41.
25. Zar S, Benson MJ, Kumar D. Rectal afferent hypersensitivity and compliance in irritable bowel syndrome: Differences between diarrhoea-predominant and constipation-predominant subgroups. Eur J Gastroenterol Hepatol 2006;18:151–8.